Nonlinear chaotic lattice field theory

X Wang, S V Williams, M N Gudorf, H Liang, and P Cvitanović

School of Physics, Georgia Institute of Technology, Atlanta, GA 30332-0430, USA

E-mail: `predrag.cvitanovic@physics.gatech.edu`

28 November 2024

Abstract. Motivated by [...]

PACS numbers: 02.20.-a, 05.45.-a, 05.45.Jn, 47.27.ed

Keywords: chaotic field theory, many-particle systems, coupled map lattices, periodic orbits, symbolic dynamics, cat maps

Submitted to: *J. Phys. A: Math. Theor.*

1. Introduction

"Amazing! I did not understand a single word!"

And indeed, there is a problem of understanding what is 'chaos' [...]

We need to motivate looking at classical ϕ^k theories, I know that there is a big push for ϕ^4 in quantum field theory, so that is likely the best way to go.

2. Deterministic lattice field theory

A scalar field $\phi(x)$ over d Euclidean coordinates can be discretized by replacing the continuous space by a d-dimensional hypercubic integer lattice $\mathbb{Z}^d$, with lattice spacing a, and evaluating the field only on the lattice points [160, 164]

$$\phi_z = \phi(x)\,, \qquad\qquad x = az = \text{lattice point}\,, \quad z \in \mathbb{Z}^d\,. \tag{1}$$

A *field configuration* (here in one spatiotemporal dimension)

$$\Phi = \cdots \phi_{-3}\phi_{-2}\,\phi_{-1}\,\phi_0\,\phi_1\phi_2\phi_3\phi_4\cdots\,, \tag{2}$$

takes any set of values in system's ∞-dimensional *state space* $\phi_z \in \mathbb{R}$. A *periodic field configuration* satisfies

$$\Phi_{z+R} = \Phi_z \tag{3}$$

for any discrete translation $R \in \mathcal{L}_{\mathbf{a}}$ in the *Bravais lattice*

$$\mathcal{L}_{\mathbf{a}} = \left\{ \sum_{i=1}^{d} n_i \mathbf{a}_i \mid n_i \in \mathbb{Z} \right\} \; = \; \left\{ \mathbf{n}\,\mathbf{A} \,|\, \mathbf{n} \in \mathbb{Z}^d \right\} \tag{4}$$

where the matrix $\mathbf{A}$ whose columns are d independent integer lattice vectors $\mathbf{a}_j$

$$\mathbf{A} = [\mathbf{a}_1, \cdots, \mathbf{a}_d] \in \mathbb{R}^{d\times d} \tag{5}$$

defines a *Bravais cell* basis.

The volume of (i.e., the number of lattice sites within) $\mathcal{L}_{\mathbf{a}}$ is defined by the volume of the parallelepiped spanned by the Bravais cell basis

$$N_{\mathbf{a}} \equiv |\det \mathbf{A}| \,. \tag{6}$$

For example, the periodic orbit for the 1D ϕ^3, $\overline{101}$, reoccurs for the discrete translation $R = 3$ and this is the only (one dimensional) vector in $\mathcal{L}_{\mathbf{a}}$ so we get the obvious answer that $N_{\mathbf{a}} = 3$ i.e. there are three points in the Bravais cell of this orbit.

The action in (**??**) is given as Bravais cell sum over the Lagrangian density

$$S_{\mathbf{a}}[\Phi] = \sum_{z}^{\mathbf{a}} \left\{ \frac{1}{2} \sum_{\mu=1}^{d} (\partial_\mu \phi)_z^2 + V(\phi_z) \right\} \,, \tag{7}$$

The variational extremum condition (8)

$$F[\Phi_c]_z = \frac{\delta S[\Phi_c]}{\delta \phi_z} = 0 \,, \tag{8}$$

yields the Euler–Lagrange equations of ϕ^k theory (50) on a d-dimensional hypercubic lattice, with *periodic state* Φ_c a global deterministic (or 'classical') solution satisfying this local extremal condition on every lattice site z.

Here, and in papers I and II [55, 137] we investigate spatiotemporally chaotic lattice field theories using as illustrative examples the d-dimensional hypercubic lattice (1) discretized Klein-Gordon free-field theory, spatiotemporal cat, spatiotemporal ϕ^3 theory, and spatiotemporal ϕ^4 theory, defined respectively by Euler–Lagrange equations (8)

$$-\Box\,\phi_z \;+\; \mu^2 \phi_z \qquad\qquad = 0 \,, \qquad \phi_z \in \mathbb{R} \,, \tag{9}$$

$$-\Box\,\phi_z \;+\; \mu^2 \phi_z - m_z \quad\;\, = 0 \,, \qquad \phi_z \in [0,1) \tag{10}$$

$$-\Box\,\phi_z \;+\; \mu^2\,(1/4 - \phi_z^2) = 0 \,, \tag{11}$$

$$-\Box\,\phi_z \;+\; \mu^2(\phi_z - \;\phi_z^3) \;\; = 0 \,. \tag{12}$$

For free-field theory the sole parameter μ^2 is known as the Klein-Gordon (or Yukawa) mass. The anti-integrable form [12, 13, 196] of the spatiotemporal ϕ^3 (11) and spatiotemporal ϕ^4 (12) Euler–Lagrange equations, and a rescaling away of other 'coupling' parameters, is explained below, in sections 8 and 9.

Each periodic state is a distinct deterministic solution Φ_c to the discretized Euler–Lagrange equations (8), so its probability density is a $N_{\mathcal{L}}$-dimensional Dirac delta function (that's what we mean by the system being *deterministic*), a delta function per site ensuring that Euler–Lagrange equation (8) is satisfied everywhere, with probability

$$P_c = \frac{1}{Z}\int_{\mathcal{M}_c} d\Phi\,\delta(F[\Phi])\,, \qquad \Phi_c \in \mathcal{M}_c\,, \tag{13}$$

where $\mathcal{M}_c$ is an open neighborhood, sufficiently small that it contains only the single periodic state Φ_c.

In [137] we verify that this definition agrees with the forward-in-time Perron-Frobenius probability density evolution [54]. However, we find field-theoretical formulation vastly preferable to the forward-in-time formulation, especially when it comes to higher spatiotemporal dimensions [55].

n-point correlation functions or 'Green functions' [185]

$$\langle \phi_i \phi_j \cdots \phi_\ell \rangle = \frac{1}{Z[0]}\int D\phi\,\mathrm{e}^{-S[\phi]}\phi_i\phi_j\cdots\phi_\ell\,. \tag{14}$$

The deterministic field theory partition sum has support only on lattice field values that are solutions to the Euler–Lagrange equations (8), and the partition function (**??**) is now a sum over configuration state space (2) *points*, what in theory of dynamical systems is called the 'deterministic trace formula' [53],

$$Z[0] = \sum_c P_c = \sum_p \sum_{r=1}^{\infty} P_{p^r}\,, \qquad P_c = \frac{1}{|\mathrm{Det}\,\mathcal{J}_c|}\,, \tag{15}$$

and we refer to the $[N_\mathcal{L}\times N_\mathcal{L}]$ matrix of second derivatives

$$(\mathcal{J}_c)_{z'z} = \frac{\delta F_{z'}[\Phi_c]}{\delta \phi_z} = S[\Phi_c]_{z'z} \tag{16}$$

as the *orbit Jacobian matrix*, and to its determinant $\mathrm{Det}\,\mathcal{J}_c$ as the *Hill determinant*. Support being on state space *points* means that we do not need to worry about potentials being even or odd (thus unbounded), or the system being energy conserving or dissipative, as long as its nonwandering periodic states Φ_c set is bounded in state space. In what follows, we shall deal only with deterministic field theory and mostly omit the subscript 'c' in Φ_c.

3. Spectrum of orbit Jacobian operator $\mathcal{J}$ on Bloch states, with examples in Cat map

To approach the spectrum of orbit Jacobian operator , it is necessary to define it "determinant" first. For some arbitray state ϕ_z, its determinant can only be considered as functional determinant (or Fredholm determinant), but in the evaluation of zeta function, a restriction of ϕ_z on periodic orbits would suffice. For a periodic state with primitive cell size n, its $\mathcal{J}$ is reduced to a $n \times n$ matrix $\mathcal{J}$, and the determinant of this matrix can be given by

$$\mathrm{Det}(\mathcal{J}) = \mathrm{Tr}_p A\mathcal{J} = \frac{1}{n}\sum_{m=1}^{n}(-1)^{m-1}(\mathrm{Tr}_{n-m}A\mathcal{J})\mathrm{Tr}\mathcal{J}^m \tag{17}$$

where A denote the anti-symmetrized tensor with $\mathrm{Tr}_0 AM = 1$. Note that $\mathrm{Tr}_i AM$ can be recursively decomposed into sum of products of $\mathrm{tr}(M^n)$ for $n \le i$. By requesting $M = \mathrm{diag}(x_1, x_2, ..., x_n)$ to be a diagonal matrix, (3) exploits all possible terms in a homogenous polynomial $p(x_1, x_2, ..., x_n)$ of degree n. But an extricate leaves only one last term. This expression of $\mathrm{Det}\mathcal{J}$ in a finite sum of traces is especially useful in the calculation of spectrum of $\mathcal{J}$, and the delicate homogeneity is especially useful when analyzing its leveled structure.

One-dimensional systems

This result was first worked out by Bountis and Helleman [30] in 1981, but their focus was on criteria of hyperbolicity, thus their calculation of spectrum was a direct decomposition of matrix. This method does not generalize to higher dimensions, so we just start out by considering the general approach based on Birdtrack formula Eq.3

For one-dimensional systems, we realize through Bloch theorem that since $r^n\mathcal{J} = \mathcal{J}$, we have $\mathcal{J}(e^{ikr}\psi_k^\alpha(r)) = \Lambda(k)^\alpha e^{ikr}\psi_k^\alpha(r)$ and the wave function $\psi_k^\alpha(r) = \psi_k^\alpha(r+n)$ has the same periodicity as underlying periodic state. In this case, one should aware that it is a wise choice to absorb all the phase into an operator $\Psi:\ \mathbb{R}^n \to \mathbb{R}^{\mathbb{Z}}$ such that $\Psi(\psi_k^\alpha(r)) = e^{ikr}\psi_k^\alpha(r)$ is extended from the primitive cell to all space with proper phase factor.

Now, to work out the spectrum of J, we still need to figure out how to put it into primitive cell so that it can be reduced to a matrix whose determinant is well-defined. To do so, we need to figure how to change order of $\mathcal{J}$ and Ψ on lattice. Write $\mathcal{J} = -r - r^{-1} + \mathbf{S}$, where $\mathbf{S}$ is a diagonal operator that commutes with Ψ, we get

$$\mathcal{J}\Psi = (-r - r^{-1} + \mathbf{S})\Psi = -\Psi r e^{ika} - \Psi r^{-1} e^{-ika} + \Phi\mathbf{S} = \Psi\mathcal{J}(k) \qquad (18)$$

where $a = 1$ should be the lattice constant and $\mathcal{J}(k)$ is the orbit Jacobian operator in primitive cell (i.e. matrix), with the shift operator r replaced by re^{ika}.

The spectrum of orbit Jacobian operator is $\prod_\alpha \Lambda^\alpha(k) = \mathrm{Det}\,\mathcal{J}(k)$ is reduced to the spectrum of a $n \times n$ matrix that suits the setup of trace calculation. As we should find immediately that $\mathrm{tr}(r^m \mathrm{S}) \neq 0$ only for $m|n$, which means that diagonal matrix S has to be put into its original position. Since we have all terms homogenous degree n, it is impossible to shift S exactly n times, so we have to make sure that shift cancels in order to contribute anything in trace. This important observation then asserts that the only term in $\mathrm{Det}\,\mathcal{J}(k)$ that depends on k should come from $\mathrm{tr}(re^{ika})^n = ne^{inka}$ and $\mathrm{tr}(re^{-ika})^n = ne^{-inka}$. Then trace calculation gives

$$\mathrm{Det}\mathcal{J}(k) = \mathrm{Det}\mathcal{J}(0) - 4\sin^2(nk/2) \qquad (19)$$

which is strikingly simple. Here we have to be aware that $\mathrm{Det}\mathcal{J}(0)$ can be negative, so upon taking the absolute value moment $sin^2(nk/2)$ term can change sign according to the sign of $\mathrm{Det}\mathcal{J}(0)$. In fig.1 I showed two spectra numerically calculated, and we can see that the prediction matches these calculations perfectly.

Higher dimensional theories, still to be worked out better

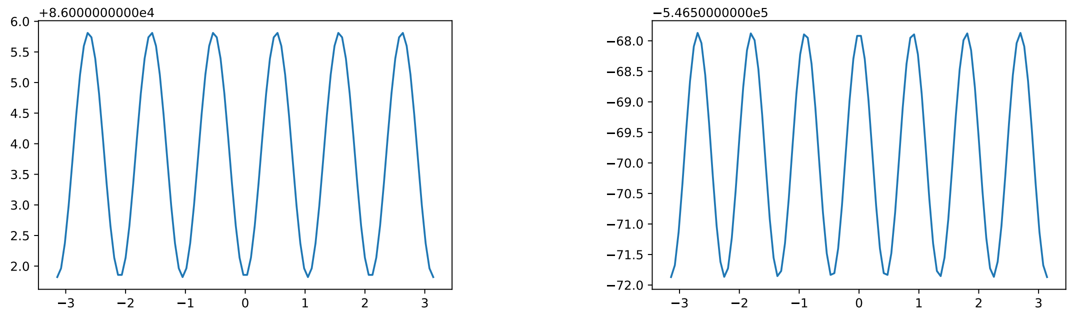

(a) (b)

Figure 1: Spectrum of $\mathcal{J}(k)$ plotted over $(-\pi, \pi)$ for an random period-6 (left) and period-7 orbit (right) for ϕ^4 theory. We can see all expected features from these figures, includes the number of peaks equal to period, even function, oscillation with amplitude $= 2$

The natural next step is to generalize this result to higher dimension, and we will first try 2-dimensional square lattice. Similar to the case in one dimension, we can absorb the phase into some operator Φ and multiply $\psi_k^\alpha(r)$ by Φ to extend primitive cell to all space. I found it convenient to define Φ_1 and Φ_2 for two dimensions separately, and clearly $r_i\Phi_j$ commutes when $i \neq j$. Thus, for a $m \times n$ 2-dimensional periodic state, the spectrum of $\mathcal{J}$ can be found by push it into the flattened $mn \times mn$ primitive cell $\mathcal{J}$, where $r_1 = r \otimes \mathbf{1}$ and $r_2 = \mathbf{1} \otimes r$. We define the primitive cell $\mathcal{J}$ to be

$$\mathcal{J}(k) = -(r_1 e^{ik_1a_1} + r_1^{-1}e^{-ik_1a_1} + r_2e^{ik_2a_2} + r_2^{-1}e^{-ik_2a_2}) + \mathrm{S} \tag{20}$$

We can still do the trace calculation, but this time it takes up power $m \times n$, and it is possible to complete multiple cycles in both direction. Then, the spectrum is now a trigonometric polynomial

$$\sum_{pm+nq \leq mn} [\sum_{n\cdot\mu=p} \sum_{m\cdot\nu=q} C(\mu,\nu) \times \prod_{i=1}^{n} \cos^{\mu_i}(imk_1) \prod_{j=1}^{m} \cos^{\nu_j}(jnk_2)] \tag{21}$$

where we define $m = (1, 2, .., m)$ and similarly $n = (1, 2, .., n)$, and we request all p, q, μ_i, ν_j to be non-negative. To reduce notation, it is more convenient to define $\langle\mu\rangle = n \cdot \mu$ and $\langle\nu\rangle = m \cdot \nu$.

To understand this formula, we have to recall the explanation of trace formula as a homogenous polynomial. Here, the independent variables are e^{imk_1}, e^{-imk_1}, e^{ink_2}, e^{-ink_2}, which form pair-wise cancellations. Due to symmetry, all of the k-dependent terms appear as $\cos(n_ik_i)$ for some direction i. And to summarize the condition for homogeneity in degrees, we separate the degree for each direction, as different directions can only possibly couple through multiplication, and their sum cannot exceed the volume of the primitive cell $m \times n$. The degree of each term $\cos(n_ik_i)$ is defined to be n_i, and in multiplication (either in the same direction or different directions), degrees add up.

In **??** we label by $mp = m\langle\mu\rangle$ the degree of k_1 terms and $nq = n\langle\nu\rangle$ the degree of k_2 terms, and each is composed by product of different modes specified by vector μ, ν. This exponential decay in **??** is an exponential in the total degree of each term, and clearly the constant term, with degree zero, is the most dominant. I took the product to be upper-bounded by n and m respectively because the superposition of the fundamental modes up to these numbers (which is essentially V/n_i) would have reached the volume of the primitive cell.

Although this spectrum is much more complicated than that for one dimension, it still gives us good intuition. First of all, we can see that this spectrum is dominated by the constant part. Then, if we look at the next level of contribution in k_1 and k_2, we can see that the direction with the shorter period dominates its longer counterpart. Finally, this spectrum is an even function for both wave numbers, and the crossing term of k_1 and k_2 comes first with $k_1^2 k_2^2$, the fourth order term. This means that in continuous limit, we should be able to decorelate perturbation in different directions. For even higher dimensions, we only need to introduce more sets of vector subscripts, and clearly all of the observations made above generalize to arbitrarily high dimensions.

To get a feeling for this 2D $\mathcal{J}$ spectrum, it is better to work out an example. We first compare the $[2\times 2]_0$ state and $[2\times 3]_0$ states of cat map with constant stretching. First, we list all possible modes for each case, which is not very hard (7 terms for $[2\times 2]_0$ and 10 terms for $[2\times 3]_0$)

$$
\begin{aligned}
&[2\times 2]_0 : && (22)\\
&\qquad \cos(2k_1), \cos(2k_2), && (23)\\
&\qquad \cos(2k_1)^2, \cos(2k_2)^2, \cos(4k_1), \cos(4k_2), \cos(2k_1)\cos(2k_2) && (24)
\end{aligned}
$$

$$
\begin{aligned}
&[2\times 3]_0 : && (25)\\
&\qquad \cos(2k_1), && (26)\\
&\qquad \cos(3k_2), && (27)\\
&\qquad \cos(2k_1)^2, \cos(4k_1), && (28)\\
&\qquad \cos(2k_1)\cos(3k_2), && (29)\\
&\qquad \cos(6k_1), \cos(2k_1)\cos(4k_1), \cos(2k_1)^3, \cos(6k_2), \cos(3k_1)^2 && (30)
\end{aligned}
$$

By these two examples, we find that the structure of two-dimensional spectrum is given by high-frequency modes and their products, compared with the single fundamental frequency expression for one-dimensional spectrum. However, we have to notice that through Chebyshev polynomials (first kind), we can reduce all the high-frequency modes to a polynomial of fundamental modes. Therefore, we reduce Eq.3 to a polynomial of momentum in each direction $p_i = 2\sin^2(T_i k_i/2)$ as

$$\mathrm{Det}\mathcal{J}(k) = \mathrm{Det}\mathcal{J}(0) + \sum_{n_1 i + n_2 j \le n_1 n_2} C_{i,j} p_1^i p_2^j \tag{31}$$

This way it is easier for numerical calculation of coefficients, and I think this "momentum" form is more illustrative to compare to harmonics.

Next, we evaluate $C_{i,j}$ by undetermined coefficients and compare with numerical result. For simplicity we still evaluate $\mathcal{J}$ by Cat map, taking primitive cell to be $[2\times 3]_0$ and $s = 4.1$. Result is shown in fig.2. We can see that fig.2a shows expected trignometric dependence on k, and fig.2b shows that the error is within unity (relatively error of order 10^{-4}).

Eq.3 has a very delicate structure due to homogeneity of Eq.3, which is displayed by the dependence of coefficients $C_{i,j}$ on s, the stretching parameter. Because only Cat map admits a constant stretching, we still take Cat map as an example to illustrate this result. The analytical expression of $C_{i,j}$, with primitive cell $[2\times 3]_0$, is listed below (also plotted in fig.3), when we define $p_i = 2\sin(n_i k_i/2)$

$$[2\times 3]_0 : \tag{32}$$
$$C_{0,0} = s^6 - 9s^4 - 4s^3 + 12s^2, \tag{33}$$
$$C_{1,0} = \frac{3}{2}s^4 - 6s^2 + 6s - 2, \tag{34}$$
$$C_{0,1} = 2s^3 - 4, \tag{35}$$
$$C_{2,0} = \frac{3}{2}s^2, \tag{36}$$
$$C_{1,1} = -3s, \tag{37}$$
$$C_{3,0} = \frac{1}{2}, C_{0,2} = 1 \tag{38}$$
$$\tag{39}$$

There are a few interesting observations we can make from this result. First, the highest-order term (i.e. the term with highest power of s) is exactly volume of primitive cell minus total degree on the term of all $C_{i,j}$, and this is due to homogeneity. In principle, we should only lower order terms that has the same parity as the highest-order term, but due to the recursive simplification we introduce some odd powers in Chebyshev polynomials, but this is just a minor detail. The important thing is that the spectrum of $\mathcal{J}$ is exponentially dominated by lower order terms in the anti-integrable limit, and is important when we evaluate the zeta function convergence in two dimensions.

Another interesting observation can be made from half-integer terms, as most of the terms in each $C_{i,j}$ admit integer coefficients. After calculating the coefficients for different primitive cells we found that all half-integer terms are related to the direction where periodicity is 2, and most coefficients in these directions (not all) have a half-integer term in its highest order. Currently we have not yet come to a conclusion to this

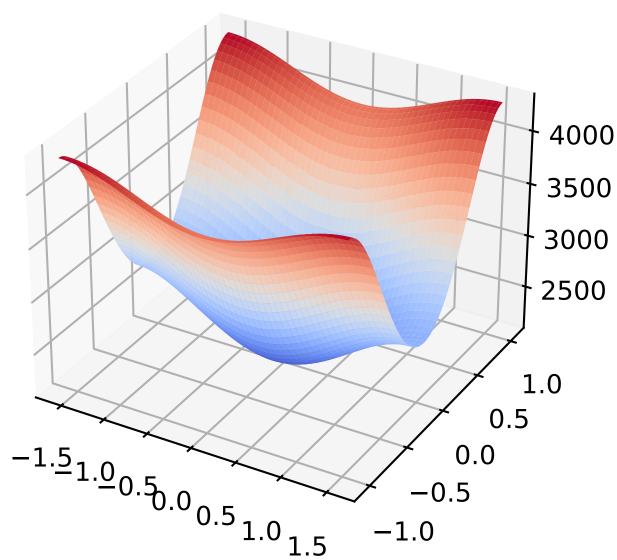

(a) Spectrum of $\mathcal{J}(k)$ evaluated by the method of undetermined coefficients

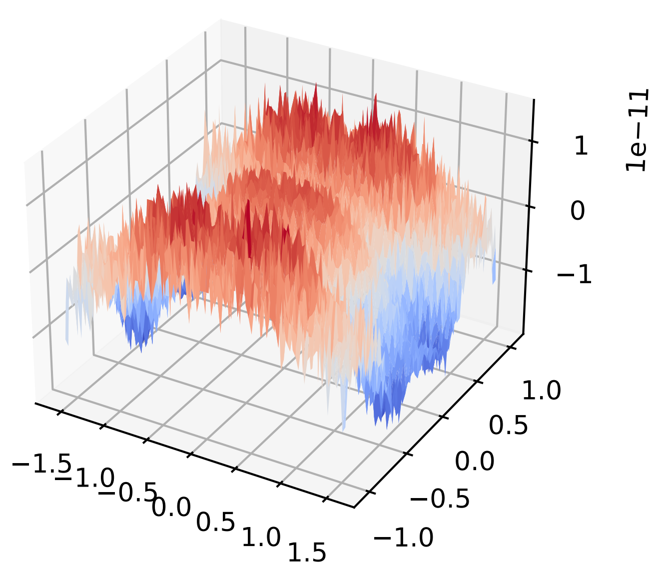

(b) Plotted difference of result in fig.2a with numerical

Figure 2: Spectrum calculation of $\mathcal{J}(k)$ for Cat map $[2 \times 3]_0$ $s = 4.1$ plotted over primitive cell

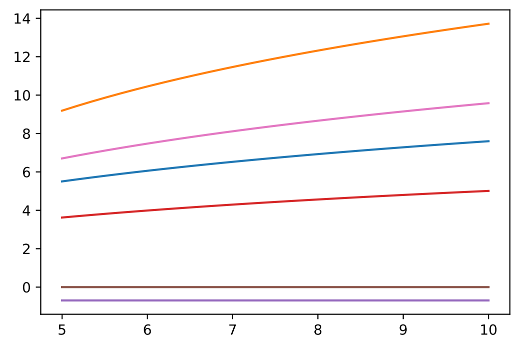

Figure 3: Plotted the dependence of $C_{i,j}$ (in log scale) on s over range $s \in [5, 10]$ for Cat map $[2 \times 3]_0$, with 7 coefficients in total

question, as Chebyshev polynomials should be unaware of the change in independent variable.

To draw a conclusion to this, we found that Eq.3 is very efficient in evaluating spectrum of $\mathcal{J}$ by providing the structure based on k dependence in higher dimensions. However, due to some detours in recursive simplification, in most case the coefficients have to be numerically evaluated, and thus this result is semi-analytical or quasi-analytical in more than one dimension. The insight provided by Eq.3 enables us to write the spectrum of $\mathcal{J}$ into Eq.3, which is previously unthinkable. This result already demonstrated its power in evaluation of one-dimensional zeta function, but we believe that it will add more to two-dimensional case.

4. Orbit stability

Solutions of a nonlinear field theory are in general not translation invariant, so the orbit Jacobian matrix (16) (or the 'discrete Schrödinger operator' [30, 191])

$$\mathcal{J}_c = \begin{pmatrix} s_0 & -1 & 0 & 0 & \cdots & 0 & -1 \\ -1 & s_1 & -1 & 0 & \cdots & 0 & 0 \\ 0 & -1 & s_2 & -1 & \cdots & 0 & 0 \\ \vdots & \vdots & \vdots & \vdots & \ddots & \vdots & \vdots \\ 0 & 0 & 0 & 0 & \cdots & s_{n-2} & -1 \\ -1 & 0 & 0 & 0 & \cdots & -1 & s_{n-1} \end{pmatrix} \tag{40}$$

is not a circulant matrix: each periodic state Φ_c has its own orbit Jacobian matrix $\mathcal{J}_c = \mathcal{J}[\Phi_c]$, with the 'stretching factor' $s_t = V''(\phi_t) + 2$ at the lattice site t a function of the site field ϕ_t.

The orbit Jacobian matrix of a period-(mn) periodic state Φ, which is a m-th *repeat* of a period-n prime periodic state Φ_p, has a tri-diagonal block circulant matrix form that follows by inspection from (40):

$$\mathcal{J}_{p^r} = \begin{pmatrix} \mathbf{s}_p & -\mathbf{r} & & & -\mathbf{r}^\top \\ -\mathbf{r}^\top & \mathbf{s}_p & -\mathbf{r} & & \\ & \ddots & \ddots & \ddots & \\ & & -\mathbf{r}^\top & \mathbf{s}_p & -\mathbf{r} \\ -\mathbf{r} & & & -\mathbf{r}^\top & \mathbf{s}_p \end{pmatrix}, \tag{41}$$

where block matrix $\mathbf{s}_p$ is a $[n\times n]$ symmetric Toeplitz matrix

$$\mathbf{s}_p = \begin{pmatrix} s_0 & -1 & & & 0 \\ -1 & s_1 & -1 & & \\ & \ddots & \ddots & \ddots & \\ & & -1 & s_{n-2} & -1 \\ 0 & & & -1 & s_{n-1} \end{pmatrix}, \quad \mathbf{r} = \begin{pmatrix} 0 & \cdots & 0 \\ & & \\ & \ddots & \vdots \\ & & \\ 1 & & 0 \end{pmatrix}, \tag{42}$$

and $\mathbf{r}$ and its transpose enforce the periodic bc's. This period-(mn) periodic state Φ orbit Jacobian matrix is as translation-invariant as the temporal cat, but now under Bravais lattice translations by multiples of n. One can visualize this periodic state as a tiling of the integer lattice $\mathbb{Z}$ by a generic periodic state field decorating a tile of length n. The orbit Jacobian matrix $\mathcal{J}$ is now a block circulant matrix which can be brought into a block diagonal form by a unitary transformation, with a repeating $[n\times n]$ block along the diagonal.

5. Observables

Because of the dependence of the orbit Jacobian matrix (41) on the primitive cell $\mathbf{A}$ repeat number r, we have to distinguish the partition function $Z_\mathbf{A}$ defined over the finite lattice volume $N_\mathcal{L} = N_\mathbf{A}$ primitive cell from the (infinite) lattice partition function $Z_\mathcal{L}$, which is the sum over all distinct primitive cells. A field configuration Φ over a primitive cell $\mathbf{A}$ of lattice $\mathcal{L}$ occurs with probability density

$$P_\mathbf{A}[\Phi] = \frac{1}{Z}\,\mathrm{e}^{-S_\mathbf{A}[\Phi]}, \qquad Z = Z_\mathcal{L}[0]. \tag{43}$$

Here $Z_\mathcal{L}$ is a normalization factor, given by the *partition sum*, the sum (in continuum, the integral) over probabilities of all configurations,

$$Z_\mathcal{L}[\mathsf{J}] = e^{N_\mathcal{L} W_\mathcal{L}} = \int_\mathcal{L} d\Phi\, P[\Phi]\, e^{\Phi\cdot\mathsf{J}}, \qquad d\Phi = \prod_z^\mathcal{L} d\phi_z, \tag{44}$$

where $\mathsf{J} = \{j_z\}$ is an external source j_z that one can vary site by site, and $S[\Phi]$ is the action that defines the theory (discussed in more detail in section **??**). The dimension of the partition function integral equals the number of lattice sites $N_\mathcal{L}$, i.e., the lattice volume (6).

Birkhoff sum [130] over primitive cell c

$$A_c = \sum_{z\in c} a_z. \tag{45}$$

Birkhoff average over primitive cell c

$$\langle a \rangle_c = \frac{A_c}{N_c} \,. \tag{46}$$

The free energy (the large-deviation potential?)

$$\begin{aligned} Z_{\mathbf{A}}[0] &= \sum_c e^{N_{\mathcal{L}} W_c[0]} \\ e^{N_{\mathcal{L}} W_c[0]} &= \int_{\mathcal{M}_c} d\Phi\, \delta(F[\Phi]) \;=\; \frac{1}{|\mathrm{Det}\, \mathcal{J}_c|} \end{aligned} \tag{47}$$

was originally snuck into (15) (see (??), (??), (??)) See also partition function (??), (??), (??); partition sum (??); Ising (??); Gaussian (??).

6. Nonlinear lattice field theory

As we are writing this as a primer to our methods geared towards nonlinear lattice field theories, we choose to consider the most structurally simple of nonlinearities: Euclidean ϕ^k theory. First, we examine a continuum scalar, one-component field, d-dimensional Euclidean ϕ^k theory defined by action [121, 179, 216]

$$S[\Phi] = \int d^d x \left\{ \frac{1}{2} \left[\partial_\mu \phi(x)\right]^2 + \frac{\mu^2}{2}\, \phi^2(x) - \frac{g}{k!}\, \phi^k(x) \right\} , \tag{48}$$

with the Klein-Gordon mass $\mu \geq 0$, and the strength of the self-coupling $g \geq 0$. When working with nonlinear systems, we are really only interested in unstable orbits. As this is the case, we have chosen our action to have the ϕ^k potential inverted when compared to more classical treatments.

When working on a discretized ϕ^k theory, the action is defined as the lattice sum over the Euclidean Lagrangian density and (48) becomes [163]

$$S[\Phi] = \sum_z \left\{ \frac{1}{2} \sum_{\mu=1}^{d} (\partial_\mu \phi)_z^2 + \frac{\mu^2}{2}\, \phi_z^2 - \frac{g}{k!}\, \phi_z^k \right\} , \tag{49}$$

where we have set lattice constant $a = 1$ throughout. In the spirit of anti-integrability [13], we split the action into 'kinetic' and local 'potential' parts $S[\Phi] = -\frac{1}{2}\Phi^\top \Box \Phi + V[\Phi]$, where the nonlinear self-interaction is contained in

$$V[\Phi] = \sum_z V(\phi_z) \,, \qquad V(\phi) = \frac{1}{2}\, \mu^2\, \phi^2 - \frac{g}{k!}\, \phi^k \,, \quad k \geq 3 \tag{50}$$

with $V(\phi_z)$ a nonlinear potential, intrinsic to the lattice site z. The part bilinear in fields is the free field theory action

$$S_0[\Phi] = \frac{1}{2} \Phi^\top \left(-\Box + \mu^2 \mathbb{1}\right) \Phi \,, \tag{51}$$

Here the lattice Laplacian

$$\Box\, \phi_z = \sum_{||z'-z||=1} (\phi_{z'} - \phi_z) = -2d\, \phi_z + \sum_{||z'-z||=1} \phi_{z'} \quad \text{for all } z, z' \in \mathcal{L} \tag{52}$$

is the average of the lattice field variation $\phi_{z'} - \phi_z$ over the sites nearest to the site z. For a hypercubic lattice in one and two dimensions this discretized Laplacian is given by

$$\Box\,\phi_t \;= \phi_{t+1} - 2\,\phi_t + \phi_{t-1} \tag{53}$$

$$\Box\,\phi_{jt} = \phi_{j,t+1} + \phi_{j+1,t} - 4\,\phi_{jt} + \phi_{j,t-1} + \phi_{j-1,t}\,. \tag{54}$$

As we have now defined an action, we can write down the lattice Euler Lagrange equation which we can solve with periodic boundary conditions in order to determine the periodic orbits central to our theories of nonlinear dynamics.

First, we note that $\Box \equiv -\partial^T\partial$ because $\Box$ is the lattice Laplacian which, in finite difference notation, is given by $\Box = \frac{1}{a^2}\left(\sigma^{-1} - 2I - \sigma\right)$ and $\partial^T\partial = \frac{1}{a^2}\left(\sigma^{-1} - I\right)\left(\sigma - I\right) = \frac{1}{a^2}\left(2I - \sigma - \sigma^{-1}\right)$ Where σ is a matrix which rotates the lattice state forward by one lattice point. Now, if we take.

$$\left(\partial_\mu\phi\right)^T\partial_\mu\phi = \phi\partial_\mu^T\partial_\mu\phi = -\phi\Box\phi \tag{55}$$

Using (55) we can write our action (49) as

$$S[\phi] = \sum_\mu \frac{1}{2}\left(\partial_\mu\phi\right)^2 + V(\phi) = \sum_\mu -\frac{1}{2}\phi\Box\phi + V(\phi) \tag{56}$$

This should encompass all our Hamiltonian field theories (those that are non-dissipative can be treated through an action formulation). Now, the functional derivative commutes with the partial derivatives present in $\Box$, and $\Box$ is self-adjoint, so it works the same acting from the right as it does acting from the left. Therefore, we can write

$$\frac{\delta S[\phi]}{\delta\phi} = \sum_\mu -\frac{1}{2}\phi\Box - \frac{1}{2}\Box\phi + V'(\phi) = 0 \tag{57}$$

Summing over independent directions to get zero implies that each member of the sum is zero, so we get

$$-\Box\phi + V'(\phi) = 0 \tag{58}$$

as our lattice Euler–Lagrange equations.

We will be closely investigating two ϕ^k theories: the aforementioned ϕ^4, and ϕ^3. ϕ^4 has wide application in quantum field theory needs citations and thus understanding its behavior from a nonlinear dynamics perspective would be extremely useful. ϕ^3 on the other hand, is less useful for qft due to the non-normalizability of its potential, but its close connection to the well-studied temporal Hénon (Appendix A) allows us to explore many properties analytically, and even draw global conclusions about our field theory formulation in general. This paper will exclusively concern itself with one-dimensional theories, this follows along with our effort to build up understanding of chaotic spatiotemporal field theories in chunks cite LC21 and CL18. In the following sections we develop both ϕ^3 and ϕ^4 from (49), some general properties of each theory are developed followed by a discussion on "shadow states" and the symmetries of each system. With all this information, we are able to use Newton's method to extremely accurately and quickly determine cycles of up to length ?? for each theory.

7. Dynamics in state space

Before discussing global properties for non-linear systems, it is conventional to take a dynamical point of view and start with local forward-in-time formulation in state space. Later this notion of local will be connected with a global picture.

Field theory is closely related with the study of dynamical system. However, such connection is not always clearly illustrated. Thus, a rigorous and detailed discussion of underlying mathematics is favorable here.

7.1. Preliminary definitions

To conform with tradition in dynamical system, let $\mathcal{M}$ be state space that contains all possible field values, and $f : \mathcal{M} \times \mathcal{M} \to \mathcal{M}$ a self-homeomorphism on $\mathcal{M}$ is corresponding discrete time evolution operator that satisfies semi-group property of time evolution, which is defined inductively

$$f^n = f \circ f^{n-1}$$
$$f^0 = id_{\mathcal{M}} \,.$$

In such a system $(\mathcal{M}, f)$, an invariant subset $A \subset \mathcal{M}$ is a set such that

$$f(A) = A \tag{59}$$

Examples of invariant subset are fixed points, limit cycles (as periodic orbits), ω-limits, etc. These invariant subsets has drawn great attention in the study of complicated dynamical systems. Among them, the most helpful ones are stable (unstable) manifolds, which are defined based on fixed points,

$$W^s(f,p) = \{q \in \mathcal{M} | f^n(q) = p, n \to \infty\}$$
$$W^u(f,p) = \{q \in \mathcal{M} | f^{-n}(q) = p, n \to \infty\} \,,$$

where superscripts s and u indicates stable and unstable respectively. In other words, stable/unstable manifolds are points attracted or repelled by the fixed point p. Anastassiou *et al* [7] used parameterization method to visualize stable/unstable manifolds for ϕ^4 theory and calculated homoclinic tangency. Locally near fixed points, the stable/unstable manifolds are locally straightened near fixed points with slopes determined by eigenvectors of Jacobian matrix (which is very reasonable as they agree in the tangent space at fixed points).

As introduced by Birkhoff[??] to strictly define dissipative systems, non-wandering set has been another important invariant subset in open systems where some solutions 'escape' from $\mathcal{M}$ and never return. The non-wandering set is defined as the complement of wandering set []. A point $x_0 \in \mathcal{M}$ is wandering if there exists a positive integer $N \in \mathbb{N}$ such that

$$\exists U \ni x_0,\ f^n(U) \cap U = \emptyset \ \forall n > N \tag{60}$$

which means that after finitely many iterations, this neighborhood of x is never visited by this given solution anymore (similar to transitive solution in Markov process). Thus, the wandering set $\mathcal{W}$ is defined as

$$\mathcal{W} = \{x \in \mathcal{M} | x \text{ is wandering } \} \tag{61}$$

Correspondingly, the non-wandering set can be defined as $\mathcal{N} = \mathcal{M} \setminus \mathcal{W}$. In fact, non-wandering set of an open system is usually extremely complicated as zero-measure fractal with empty interior [53]. However, a finite-level rough visualization is available by the idea of Smale's horseshoe map. The usual practice is to take a large enough square cover near origin and map it forward and backward in time to intersect itself. Nevertheless, this practice seems rather artificial, since a square is in no way natural to the dynamics. A better approach is the find cover that is bounded by invariant manifolds instead (referred to as optimal cover later). This method is demonstrated using example of ϕ^3 and ϕ^4 in the following section.

In strong coupling regime, many physically important systems are characterized mathematically by Axiom A, which satisfies:

(i) $\Omega(f)$is compact

(ii) The set of periodic point is dense in$\Omega(f)$

For any surface, hyperbolicity of non-wandering implies density, thus sometimes hyperbolic and axiom A are used interchangeably. The density of Axiom A diffeomorphism ensures that there exists an open neighborhood of $U \supset \Omega(f)$ and

$$\Omega(f) = \bigcap_{z \in \mathrm{Z}} f^z(U) \tag{62}$$

is a locally maximal invariant set for f. This is important for visualization technique of non-wandering set. An Axiom A diffeomorphism also supports a Markov partition [31] that lays basis for definition of symbolic dynamics.

As another important dynamical concept, hyperbolicity is characterized by local properties of tangent bundle. A differentiable map f is said to have hyperbolic structure on subset $\Lambda \subset \mathcal{M}$ if its tangent space can be decomposed into a direct sum of contracting and expanding directions at every point in Λ. Formally, Λ is a hyperbolic set if $\forall x \in \Lambda$,

$$
\begin{aligned}
&(i) \quad T_x M = E_x^s \bigoplus E_x^u \\
&(ii) \quad d_x f(E_x^{s,u}) = E_{f(x)}^{s,u} \\
&(iii) \, |d_x f|_{E_x^s} < \lambda_1, \; |d_x f^{-1}|_{E_x^u} < 1/\lambda_2, \; (0 < \lambda_1 < 1 < \lambda_2) \,,
\end{aligned}
$$

which means that $E_x^{s,u}$ are subspaces that are invariant under differential of f and represent contraction and expansion respectively.

7.2. Dynamical formulation on non-linear field theories

Such formal discussion of dynamical systems would be meaningless if we cannot associate the non-linear field theories of interest a dynamical formulation. Indeed, it is as natural as the transition from Lagrangian to Hamiltonian for any field theories at hand. Limiting ourselves on the highly nontrivial one-dimensional deterministic field theories, state space is $\mathcal{M} = \mathbb{R}^2$ due to three-term recurrence relation of ϕ^3 and ϕ^4(ref). Any point (represent a unique orbit) in $\mathcal{M}$ can be thought as given by it initial conditions (ϕ_0, ϕ_1) or (ϕ_0, φ_0) where $\varphi_t = \phi_{t+1}$. Time evolution is given by field equation $\phi_{t+1} = g(\phi_t, \phi_{t-1})$, written in vector form as

$$\hat{f}(\hat{\phi}_t) = \hat{f}\,(\,\varphi\,)_t \qquad \phi_t = (\,\phi\,)_t \qquad g(\phi_t, \varphi_t) = (\,\phi\,)_t \qquad \phi_{t+1} = \hat{\phi}_{t+1} \tag{63}$$

This operator $\hat{f}$ is completely specified by $g : \mathbb{R}^2 \to \mathbb{R}$, and for ϕ^3 and ϕ^4 it is given by

$$\begin{aligned} g(\phi_t, \phi_{t-1}) &= -\phi_{t-1} + \mu^2(-1/4 + \phi_t^2) + 2\phi_t \quad (\phi^3) \\ g(\phi_t, \phi_{t-1}) &= -\phi_{t-1} - \mu^2\phi_t^3 + (\mu^2 + 2)\phi_t \quad (\phi^4) \end{aligned} \tag{64}$$

This dynamical formulation gives a way to look at local properties like Jacobian matrix $\mathbb{J}$ or to inspect conditions for hyperbolicity in non-linear field theories. As temporal ϕ^3 theory is conjugate to the famous Henon map, studies on sufficient condition of hyperbolicity had been rich, and we just take result $a > 5.699310786700...$, which correspond to $\mu^2 > 5.17661....$ This makes us take $\mu^2 = 5.5$ for the rest discussion on ϕ^3 theory. In case of ϕ^4 theory, although it has attracted much attention in quantum field theory, the dynamical counterpart of ϕ^4 theory (which is a cubic map) is not as well investigated as Hénon, but a lot of efforts has been devoted to find a lower bound, similar to the bound of parameter a given. We adopt criterion from (ref) and take $\mu^2 = 3.5$ for our discussion on ϕ^4 theory, whose hyperbolicity can also be shown graphically in the next section through the existence of a transversal homoclinc point.

7.3. Homoclinic tangle

Another important insight from dynamical system is homoclinic tangle, first proposed by Poincare to account for the complicated behavior of evolution operator. More speficially, Smale-Birkhoff theorem suggests that the existence of a transversal homoclinic point implies the existence of an invariant Cantor set, and the dynamics on which is topologically conjugate to a m-symbol full shift. This notion of m-symbol full shift was later formalized by Smale as symbolic dynamics.

Compare to the mathematically rigorous discussion of existence of non-wandering set, this homoclinic tangle is much more intuitive, as it can be visualized through invariant manifolds , but we insisted that a detailed description of hyperbolicity and Axiom-A is necessary, as they can promote a natural way to visualize non-wandering set through intersections of a cover U of the non-wandering set. Here we propose a cover that is dynamically determined by the system, which we will call optimal cover in the following discussion.

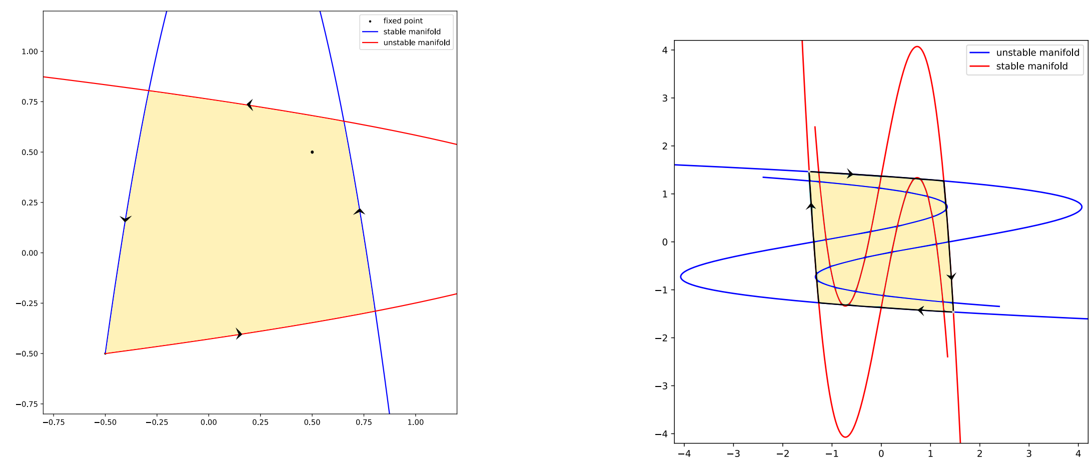

(a) Optimal cover of ϕ^3 theory with $\mu^2 = 5.5$

(b) Optimal cover of ϕ^4 theory with $\mu^2 = 3.5$

Figure 4: Visualization of optimal covers for ϕ^3 and ϕ^4 theory. Blue color indicates unstable manifold; red color indicates stable manifold; arrows indicates direction of expansion and contraction of invariant manifolds under time evolution f.

7.4. Visualizing non-wandering set for ϕ^3 and ϕ^4

The key construction of an optimal cover of non-wandering set is to find a region that covers non-wandering set and whose boundary is invariant. This case is clearly illustrated by ϕ^3 example in Fig.4a, where the optimal cover is a region bounded by stable and unstable manifolds of fixed point origin. For ϕ^4, it is more complicated, as stable and unstable manifold from any of the fixed points cannot bound the non-wandering set. However, considering the internal symmetry ($\phi \to -\phi$) exhibited by ϕ^4 potential, invariant manifolds are not the only invariant subset that can serve as boundary. Period-2 orbits are pairwise degenerated after quotient of internal symmetry, and a union of their corresponding invariant manifolds (which can be thought as manifolds for evolution f^2) is also an invariant subset of M under f. Thus, for ϕ^4, optimal cover is bounded by the invariant manifolds associated with period 2 orbits, as illustrated in Fig.4b.

With the given optimal cover, approximation of non-wandering set follows 'bend and intersection' procedure of Smale's horseshoe map [], where diffeomorphism f is time evolution operator. Schematic plots Fig.5a Fig.**??** show how optimal covers are bent through a "stretch and fold" process.

The conjugation of time evolution in Ω and a m-symbol full-shift is manifested by a closer look at $f(N) \cap N$ and $f^{-1}(N) \cap N$ in Fig.5. In general, time evolution of ϕ^k theory conjugates to k-1 symbols, as $f(N)$ is divided by N into k-1 simply connected regions in $\mathbb{R}^2$ where k-1 symbols can be assigned, the construction of which is reminiscent

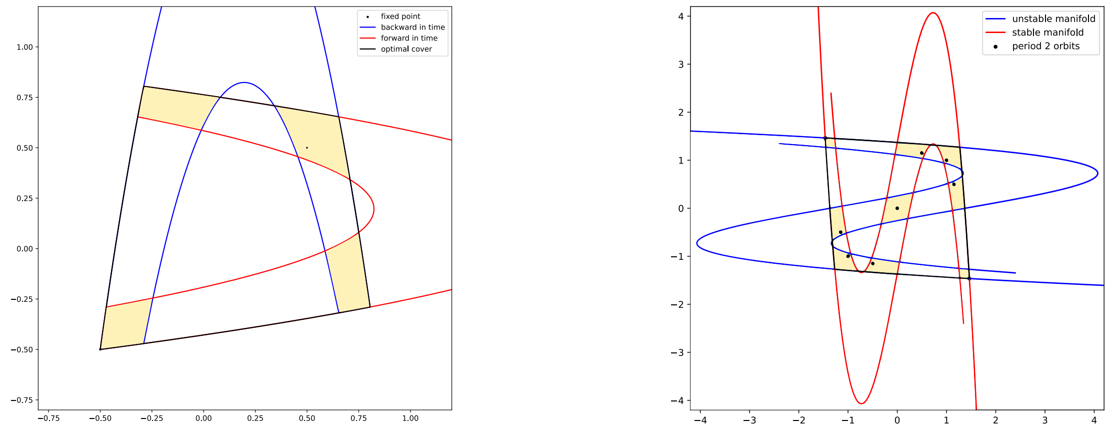

(a) "Stretch & fold" dynamics of ϕ^3 theory with $\mu^2 = 5.5$

(b) "Stretch & fold" dynamics of ϕ^4 theory with $\mu^2 = 3.5$

Figure 5: Schematics plots of how Ω is constructed through a dynamical process topologically equivalent to Smale's horseshoe

of Cantor set. Following the time evolution, $f^2(N) \cap N$ consists of $(k-1)^2$ simply-connected regions, with each region represented by a length-2 string with k-1 symbols, and $f^n(N) \cap N$ $(k-1)^n$ regions represented by length-n strings. Thus, we construct a sequence of nested sets (as finite approximations of Ω) $\{\Omega_n\}$ such that

$$\Omega_n = (f^n(N) \cap N) \cap (f^{-n}(N) \cap N), \quad (\Omega_n \subset \Omega_{n'} \forall n > n') \tag{65}$$

The structure of invariant set (which is the limit of this nested sequence) $\Omega = \lim_{n\to\infty} \bigcap \Omega_n$ is revealed by the sequence of $\{\Omega_n\}$. Write $\Omega_n = (f^n(N) \cap N) \cap (f^{-n}(N) \cap N)$, it is clear that $f^n(N) \cap N$ resembles the construction of Smale's horseshoe map, where the existence of a transversally homoclinic point guarantees that $f^n(N) \cap N$ is a disjoint union of $(k-1)^n$ simply connected regions (for ϕ^k theory, with our example taking $k = 3, 4$), each being compact. Therefore, we can label the $(k-1)^{2n}$ disjoint connected regions in Ω_n (as an intersection of $f^n(N) \cap N$ and its reversed image) by a length 2n string with $k-1$ symbols.

$$\Omega_n = \bigsqcup_{s \in S_n} \Omega_n^s \,, \; S_n = \mathcal{A}^{2n} \,, \; |\mathcal{A}| = k - 1 \tag{66}$$

We arrange the symbol strings in such a way that if $s = s_{-n+1}s_{-n+2}...s_0s_1...s_n$ and $s' = s'_{-m+1}s'_{-m+2}...s'_0s'_1...s'_m$ $(n > m)$ and $s_k = s'_k$ $(\forall |k| \leq m)$, then $\Omega_n^s \subset \Omega_m^{s'}$ (which is possible because $\{\Omega_n\}$ is a nested sequence). Notice that we construct a Markov partition $\{\Omega_n^s\}_{s \in S_n}$ at each finite approximation Ω_n, which is the famous result prove by Bowen in 1975. With this arrangement, for each bi-infinite string $s = ...s_{-1}s_0s_1s_2... \in S = \mathcal{A}^{\mathbb{Z}}$, we can construct a sequence of nested compact sets $\{\Omega_n^{s^n}\}$ where $s^n = s_{-n+1}...s_0s_1...s_n$ denote the finitely truncated substring of s of length

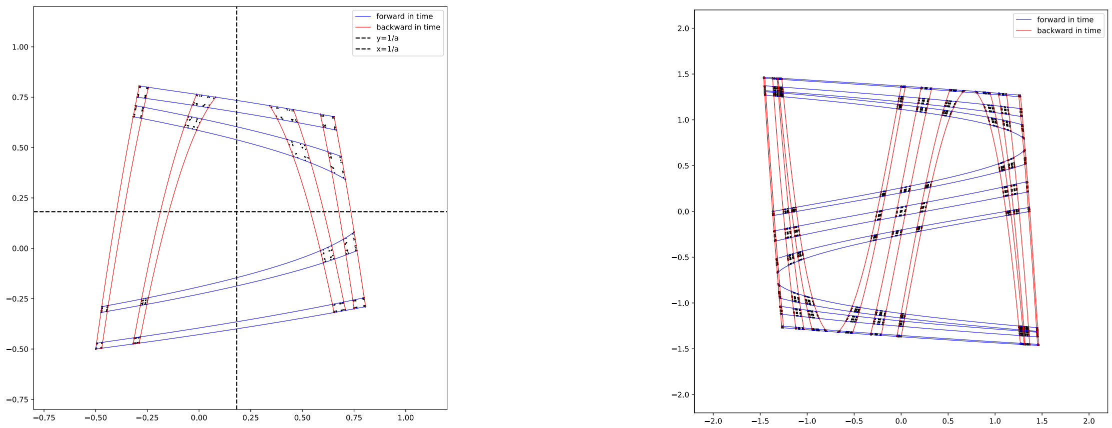

(a) Approximation of Ω_2 and P for ϕ^3 theory with $\mu^2 = 5.5$

(b) "Approximation of Ω_2 and P for ϕ^4 theory with $\mu^2 = 3.5$

Figure 6: Schematics plots of the correspondence between Ω and $\bar{P}$, where the self-similar structure of Cantor set is cleared presented

2n. Let $\Omega^s = \lim_{n\to\infty} \bigcap \Omega_n^{s^n}$, by Cantor's intersection theorem Ω^s is non-empty. Since Ω is the disjoint union of Ω^s

$$\Omega = \bigsqcup_{s\in\mathcal{A}^{\mathbb{Z}}} \Omega^s \tag{67}$$

and Ω is, by its fractal nature, a totally disconnected, whose connected components are only singletons, we conclude that every orbit in Ω is uniquely represented by a bi-infinite string in S. By far, we have constructed a bijection between Ω and S, and it is clear that the time evolution (restricted on Ω) $f|_\Omega : \Omega \to \Omega$ is represented by a shift in S (and bijection guarantees it to be a full shift).

In this process as lies the important fact $\bar{P} = \Omega$, where P is the set of all periodic solutions and the bar means closure (mathematically speaking the smallest close set that contains P). Since the "diameter" of Ω^s decreases as the length of s increases, we can conclude that in an arbitrarily small neighborhood of $x \in \Omega\backslash P$ there is a periodic solution $c \in P$. The correspondence between $\bar{P}$ and Ω (both as finite approximations) is shown in Fig.6 for both ϕ^3 (left panel) and ϕ^4 (right panel). This figure shows all periodic states up to period 7 and $f^2(N)\cap f^{-2}(N)$. There is a clear self-similar structure for these periodic orbits, and expected correspondence between these two sets is clear.

In a metric space (like $\mathbb{R}^2$), all the points $x \in \bar{P}\backslash P$ are said to have 'zero distance' with P, which means that for any $\delta > 0$, we can find $c \in P$ such that $d(x, c) < \delta$. We will say that c shadows x with precision δ. The existence of shadowing is the solid foundation of cycle expansion for dynamics zeta function, which will be thoroughly explored in the next section.

Through the visualization process, it is becomes clear that for a certain range of parameter (when homoclinic tangency exists), ϕ^k theory is an Axiom A flow and possess hyperbolicity on the locally maximal invariant set Ω. The dynamics on Ω is thus conjugated to a $k-1$ symbol full shift, and this enables us to use shadowing (i.e. exploit the properties of Ω by calculation based on P) in cycle expansion of dynamical zeta function.

8. Deterministic ϕ^3 lattice field theory

To obtain a workable ϕ^3 theory we start by considering the non-Laplacian part of the action (49), with cubic Biham-Wenzel [27] lattice site potential (50)

$$V(\phi) = \frac{\mu^2}{2}\,\phi^2 - \frac{g}{3!}\,\phi^3 = -\frac{g}{3!}\Big(\phi^3 - 3\lambda\,\phi^2\Big)\,, \quad \lambda = \mu^2/g\,, \tag{68}$$

parametrized by the Klein-Gordon mass $\mu > 0$ and the self-coupling constant $g \geq 0$.

Here we bring it to the anti-integrable [12, 13, 196] form, suitable for the analysis of theory's strong coupling limit.

We start by a field translation $\phi \to \phi + \epsilon$:

$$-\frac{g}{3!}\Big((\phi+\epsilon)^3 - 3\lambda(\phi+\epsilon)^2\Big) = -\frac{g}{3!}\Big(\phi^3 + 3(\epsilon-\lambda)\phi^2 + 3\epsilon(\epsilon-2\lambda)\phi\Big) + (\mathrm{const})\,.$$

Choose the field translation $\epsilon = \lambda$, such that the ϕ^2 term vanishes,

$$-\frac{g}{3!}(\phi^3 - 3\lambda^2\phi) + (\mathrm{const})\,.$$

Drop the (const) term, and rescale the field $\phi \to 2\,\lambda\,\phi$:

$$-4\lambda^2\mu^2\Big(\frac{\phi^3}{3} - \frac{\phi}{4}\Big)\,.$$

As the Euler-Lagrange equations are invariant to an overall constant factor, we can ignore the overall factor of $4\lambda^2$ that appears and the ϕ^3 scalar field theory action (49) takes the form

$$S[\Phi] = \sum_z \left\{-\frac{1}{2}\phi_z\Box\phi_z - \mu^2\Big(\frac{\phi_z^3}{3} - \frac{\phi_z}{4}\Big)\right\}\,. \tag{69}$$

The Euler–Lagrange equation (8) for the scalar lattice ϕ^3 field theory is now, in the $d=1$ temporal lattice case

$$-\phi_{t+1} + 2\,\phi_t - \phi_{t-1}\; - \mu^2(\phi_t^2 - 1/4) \;=\; 0\,, \tag{70}$$

and in the d-dimensional spatiotemporal lattice case,

$$-\sum_{||z'-z||=1}(\phi_{z'} - \phi_z) \;-\; \mu^2\,(\phi_z^2 - 1/4) \;=\; 0\,, \tag{71}$$

parametrized by a *single* parameter, the Klein-Gordon mass μ^2, with the “coupling constant” g in (49) scaled away.

Next, we compute the period-1 periodic states.

Period-1 periodic states. From the Euler–Lagrange equation (70) it follows that the period-1, constant periodic states, $\phi_t = \overline{\phi}$, for the $d = 1$ lattice are the zeros of function

$$F[\overline{\phi}] = \mu^2\Big(\overline{\phi}^2 - \frac{1}{4}\Big)\,, \tag{72}$$

with two real roots $\overline{\phi}_m$

$$(\overline{\phi}_L, \overline{\phi}_R) = \Big(-\frac{1}{2}, \frac{1}{2}\Big)\,. \tag{73}$$

Period-2 periodic states. To determine the four period-2 periodic states $\overline{\Phi}_m = \overline{\phi_0\phi_1}$, set $x = \phi_{2k}$, $y = \phi_{2k+1}$ in the Euler–Lagrange equation (70),

$$\mu^2(-x^2 + 1/4) + 2\,x - 2\,y \;=\; 0\,, \tag{74}$$

$$2\,\phi_1 \;+\; \mu^2(-\phi_1^2 + 1/4) - 2\phi_0 \;=\; 0\,, \tag{75}$$

and seek the zeros of

$$F[x,y] = \begin{pmatrix} -\mu^2(x^2 - 1/4) + 2\,x - 2\,y \\ -\mu^2(y^2 - 1/4) + 2\,y - 2\,x \end{pmatrix}. \tag{76}$$

That is best done using the Friedland and Milnor [84] 'the center of gravity' and Endler and Gallas [71, 72] 'center of mass' or 'orbit' polynomials, but for the period-2 periodic states it suffices to eliminate y using $F_1 = 0 \Rightarrow 2\,y(x) = -\mu^2(x^2 - 1/4) + 2x$, and seek zeros of the second component,

$$F_2[x,y(x)] = -\mu^2\Big(x - \frac{1}{2}\Big)\Big(x + \frac{1}{2}\Big)\Big(\frac{\mu^4}{4}x^2 - \mu^2 x + \Big(2 - \frac{\mu^4}{16}\Big)\Big) \tag{77}$$

The first 2 roots are the $x = y$ period-1 periodic states (73) There is one period-2 periodic state $\overline{12}$

$$x, y = \pm 2\sqrt{\frac{1}{16} - 1}\mu^4\mu^2 + \frac{2}{\mu^2}\,, \tag{78}$$

so the prime period-2 periodic state exists for $\mu^2 > 4$. For $\mu^2 = 4$ the period-2 periodic states pairs coalesce with the positive period-1 periodic states

$$F_2[x,y(x)] = -4(x^2 - \frac{1}{4})(x^2 - \frac{1}{2})^2\,. \tag{79}$$

The first two roots are the $x = y$ period-1 periodic states (73). There is one symmetric period-2 periodic state $\overline{LR}$

$$x = -y = \pm\sqrt{1{+}??/\mu^2}\,, \tag{80}$$

and a pair of period-2 asymmetric periodic states $\overline{LC}$, $\overline{CR}$ related by reflection symmetry (time reversal).

For μ^2 =?? the period-2 asymmetric periodic states pairs coalesce with the two period-1 asymmetric periodic states

$$2\,x(x^2 - 3)(x^2 - 1)^3\,. \tag{81}$$

To get a complete horseshoe (all 2^n 2-symbol unimodal map itineraries are realized), you know what to do next (see figure 2. in [84]). Numerical work indicates [215] that for $\mu^2 >??2.95$ the horseshoe is complete.

In the anti-integrable limit [12, 13] $\mu \to \infty$, the site field values

$$F_2[x, y(x)] \to \frac{\mu^8}{8}(x+??)^2\, x^? \,(x-1)^? \tag{82}$$

tend to the three steady states (89).

the orbit Jacobian matrix

$$\mathcal{J}_{zz'} = -\,\Box_{zz'} \;-\; 2\,\mu^2\phi_z\,\delta_{zz'}\,, \tag{83}$$

9. Deterministic ϕ^4 lattice field theory

Consider the discrete scalar one-component field, d-dimensional ϕ^4 theory [185] defined by the Euclidean action (49)

$$S[\Phi] = \sum_z \left\{ \frac{1}{2}\sum_{\mu=1}^{d}(\Delta_\mu\phi_z)^2 + \frac{\mu^2}{2}\,\phi_z^2 - \frac{g}{4!}\,\phi_z^4 \right\}\,, \tag{84}$$

with the Klein-Gordon mass $\mu \geq 0$, quartic lattice site potential (50),

$$V(\phi) = \frac{1}{2}\,\mu^2\,\phi^2 - \frac{g}{4!}\,\phi^4\,, \tag{85}$$

the strength of the self-coupling $g \geq 0$, and we set lattice constant $a = 1$ throughout.

For a history of ϕ^4 theories in physics, see Campbell [**Campbell19**] *Historical overview of the ϕ^4 model* (2019). Curiously, our chaotic field theory version of the ϕ^4 theory, with the 'inverted potential' sign of the μ^2 nonlinear term, seems to not be even mentioned in Kevrekidis and Cuevas-Maraver [**KevCue19**, **Campbell19**] *A Dynamical Perspective on the ϕ^4 Model: Past, Present and Future* (2019).

A popular way [145] to rewrite the quartic action (84) is to complete the square

$$V(\phi) = -\frac{g}{4!}\left(\phi_z^2 - 3!\,\frac{\mu^2}{g}\right)^2 + (\text{const})\,,$$

drop the (const) term, and rescale the field $\phi_z^2 \to 3!\,\frac{\mu^2}{g}\phi_z^2$:

$$S[\Phi] = 3!\,\frac{\mu^2}{g}\sum_z\,\left\{ -\frac{1}{2}\phi_z\Box\phi_z - \frac{1}{4}\,\mu^2\left(\phi_z^2 - 1\right)^2 \right\}. \tag{86}$$

The Euler–Lagrange equation (50) for the $d = 1$ scalar lattice ϕ^4 field theory,

$$-\phi_{t+1} + [-\mu^2\,\phi_t^3 + (\mu^2+2)\,\phi_t] - \phi_{t-1} \;=\; 0\,, \tag{87}$$

is thus parametrized by a *single* parameter, the Klein-Gordon mass $\mu^2 = s-2$, with the "coupling constant" g in (84) scaled away. Next, we compute the period-1 and period-2 periodic states.

Period-1 periodic states. From the Euler–Lagrange equation (87) it follows that the period-1 periodic states, $\phi_t = \overline{\phi}$, for the $d=1$ lattice are the zeros of function

$$F[\overline{\phi}] = \mu^2\,(1+\overline{\phi})\,\overline{\phi}\,(1-\overline{\phi})\,. \tag{88}$$

As long as the Klein-Gordon mass is positive, there are 3 real roots $\overline{\phi}_m$

$$(\overline{\phi}_L, \overline{\phi}_C, \overline{\phi}_R) = (-1, 0, 1)\,. \tag{89}$$

The period-1 Bravais cell orbit Jacobian matrix $\mathcal{J}$ is a $[1\times 1]$ matrix

$$\mathcal{J} = s_m = \frac{dF[\phi]}{d\phi} = \mu^2\,(1-3\overline{\phi}_m^2) \;=\; \mu^2 \;\text{ or }\; -2\mu^2\,, \tag{90}$$

so the "stretching" factor for the 3 steady periodic states is

$$(s_L, s_C, s_R) = (-2\mu^2, \mu^2, -2\mu^2)\,. \tag{91}$$

Period-2 periodic states. To determine the nine period-2 periodic states $\overline{\Phi}_m = \overline{\phi_0\phi_1}$, set $x=\phi_{2k}$, $y=\phi_{2k+1}$ in the Euler–Lagrange equation (87), and seek the zeros of

$$F[x,y] = \begin{pmatrix} -(s-2)x^3 + sx - 2y \\ -(s-2)y^3 + sy - 2x \end{pmatrix}. \tag{92}$$

That is best done using the Friedland and Milnor [84] 'the center of gravity' and Endler and Gallas [71, 72] 'center of mass' or 'orbit' polynomials, but for the period-2 periodic states it suffices to eliminate y using $F_1 = 0 \Rightarrow 2\,y(x) = -x^3 + sx$, and seek zeros of the second component,

$$F_2[x,y(x)] = \frac{\mu^8}{8}(x-1)\,x\,(x+1)\Big(x^2-1-\frac{4}{\mu^2}\Big)\Big(x^4-(1+\frac{2}{\mu^2})x^2+\frac{4}{\mu^4}\Big) \tag{93}$$

The first 3 roots are the $x=y$ period-1 periodic states (89). There is one symmetric period-2 periodic state $\overline{LR}$

$$x = -y = \pm\sqrt{1+4/\mu^2}\,, \tag{94}$$

and a pair of period-2 asymmetric periodic states $\overline{LC}$, $\overline{CR}$ related by reflection symmetry (time reversal).

For $\mu^2 = 2$ the period-2 asymmetric periodic states pairs coalesce with the two period-1 asymmetric periodic states

$$2\,x(x^2-3)(x^2-1)^3\,. \tag{95}$$

To get a complete horseshoe (all 3^n 3-symbol bimodal map itineraries are realized), you know what to do next (see figure 2. in [84]). Numerical work indicates [215] that for $\mu^2 > 2.95$ the horseshoe is complete.

In the anti-integrable limit [12, 13] $\mu \to \infty$, the site field values

$$F_2[x,y(x)] \to \frac{\mu^8}{8}(x+1)^3\,x^3\,(x-1)^3 \tag{96}$$

tend to the three steady states (89).

the orbit Jacobian matrix

$$\mathcal{J}_{zz'} = -\,\Box_{zz'} \;+\; \mu^2(1\,-\,3\,\phi_z^2)\,\delta_{zz'}\,. \tag{97}$$

9.1. Forward in time formulation of ϕ^4

To match with Henon's formulation of ϕ^3 theory, it is inspiring to rewrite the second order difference equation of ϕ^4 theory (87) (with 1 spatiotemporal dimension) into two first order equations. The 'two-configuration representation' (reference) $\hat{\phi}_t = (\varphi_t, \phi_t)$, where $\varphi_t = \phi_{t-1}$. Then, the forward-in-time map can be written has a system of equations

$$\phi_{t+1} = -\mu^2\phi_t^3 + (\mu^2+2)\phi_t - \varphi_t \tag{98}$$

$$\varphi_{t+1} = \phi_t \tag{99}$$

or simply in two-configuration representation

$$\hat{\phi}_{t+1} = \begin{pmatrix} \phi_t \\ -\mu^2\phi_t^3 + (\mu^2+2)\phi_t - \varphi_t \end{pmatrix} \tag{100}$$

Now, assume that a periodic solution $\Phi = \overline{\phi_1\phi_2...\phi_n}$ is given, by notation above a sequence of vectors $\left(\hat{\phi}_1, \hat{\phi}_2, ..., \hat{\phi}_n\right)$ (let $\phi_0 = \phi_n$) is associated with this solution. For a discrete dynamical system, the stability of a solution must come along with the solution to make anything meaningful. Locally, stability is represented by how neighborhood is distorted by time-forward map. A deviation with two-configuration representation is defined as

$$\Delta\phi_k = \begin{pmatrix} \Delta\varphi_k \\ \Delta\phi_k \end{pmatrix} = \begin{pmatrix} \Delta\phi_{k-1} \\ \Delta\phi_k \end{pmatrix} \tag{101}$$

Two deviation vectors (also true for non-periodic states) are associated with forward-in-time Jacobian matrix

$$\Delta\phi_{k+1} = \mathbb{J}_k \Delta\phi_k \tag{102}$$

which is defined as

$$\mathbb{J}_t = \begin{pmatrix} 0 & 1 \\ -1 & -\mu^2\phi_t^3 + (\mu^2+2)\phi_t \end{pmatrix} \tag{103}$$

For a periodic state Φ, a finite sequence of Jacobian matrices $(\mathbb{J}_1, \mathbb{J}_2, ..., \mathbb{J}_n)$. This sequence of Jacobian matrices for periodic orbits is extremely useful in calculation of cyclic expansion, and it is closely related to the stability on lattice. Dynamics of periodic orbits are evaluated by the finite product of expanding eigenvalues of this sequence (reference). Notice that matrices $\mathbb{J}_k$ depends on the lattice set given, so this other formulation doesn't turn a global non-linear theory into a linear one. However, it does make local calculation easier (if not making it possible), which will be discussed later.

10. Symbol mosaic

In the theory of dynamical systems, symbolic dynamics is a powerful tool for systematically encoding distinct temporal orbits by their symbolic itineraries. Here we briefly review the symbolic dynamics for temporal dynamical systems, then generalize this method to spatiotemporal problems, where the symbol sequences are replaced by 'mosaics', d-dimensional symbols arrays, which represent spatiotemporal periodic states globally in the spacetime [43, 44, 55, 92, 93, 149, 150].

Mosaics represents orbits by arrays of letters from a finite alphabet. Count of admissible mosaics is a convenient way to count periodic states. Consider the map of ϕ^4 field theory as an example. In section 7.2 we show that the non-wandering set of the map is bounded and the map has a three-fold horseshoe, which intersects with the optimal cover of the non-wandering set in three separated regions. The non-wandering set in the state space can be partitioned by the three strips of the horseshoe, with each region labeled by a symbol in the three-letter alphabet $\{-1, 0, 1\}$. We choose the Klein-Gordon mass μ^2 large enough such that the horseshoe of the map is complete, so every symbol sequence corresponds to one periodic orbit of the system.

Given the symbol sequences, there are many different numerical methods that can find the corresponding periodic orbits, from the simplest Newton method, to more sophisticated approaches, such as Biham and Wenzel [27] method, Hansen [95] method, Vattay [53] 'inverse iteration' method and Sterling [197] 'anti-integrable continuation' method. All of these methods require a good initial starting point, so that they converge to the periodic orbit corresponding to the given symbol sequence. A good initial point can be constructed using the symbol sequence. For the map of ϕ^4 field theory with sufficiently large μ^2, using the pseudo-orbit consists of the fixed points corresponding to the symbols in the symbol sequence is already good enough to find the periodic orbit.

For spatiotemporal dynamical systems such as the spatiotemporal cat, spatiotemporal ϕ^3 and ϕ^4 field theory, the symbolic representation of periodic states can be given by symbol arrays, instead of symbol sequences. We refer to the symbol array as the *mosaic*. For a d-dimensional spatiotemporal system, the mosaic M_c of a periodic state Φ_c is a d-dimensional symbol array:

$$\mathsf{M}_c = \{m_z\}\,, \quad m_z \in \mathcal{A}\,, \quad z \in \mathbb{Z}^d\,, \tag{104}$$

where $\mathcal{A}$ is the alphabet of the symbols. Instead of treating the spatiotemporal systems as coupled maps and partitioning the high-dimensional state space, here we assign the global symbolic mosaics using the continuation from the anti-integrable limit of the systems, following the symbolic coding of Sterling *et al* [196–198] for coupled Hénon map lattice.

Consider the spatiotemporal ϕ^3 (69) and ϕ^4 (86) as examples. At the anti-integrable limit where the Klein-Gordon mass $\mu^2 \to \infty$, the ϕ^3 and ϕ^4 field theories are no longer deterministic. The temporal and spatial coupling becomes insignificant compare to the local potential, so the local field values do not depend on their neighbors, and the periodic states of the systems are arbitrary arrays of field values from a set of anti-integrable states, $\{-1/2, 1/2\}$ for ϕ^3 theory (69), and $\{-1, 0, 1\}$ for ϕ^4 theory (86). Using the set of the anti-integrable states as the symbolic alphabet $\mathcal{A}$, Sterling *et al* [196–198] showed that for single and coupled Hénon map, every symbol mosaic M_c corresponds to an unique periodic state Φ_c which is contained in a neighborhood of M_c, providing that the system is sufficiently close to the anti-integrable limit. Applying this symbolic coding to spatiotemporal ϕ^3 and ϕ^4 field theories, we have a 2-letter alphabet for ϕ^3 theory and a 3-letter alphabet for ϕ^4 theory. In this paper we choose sufficiently large Klein-Gordon mass μ^2 such that every symbol mosaic is admissible in our desired spatiotemporal domain. The mosaics are close to the corresponding periodic states, hence they are good initial starting points for numerically finding the periodic states.

11. Symmetry

All the chaotic field theories that we have examined in this and our companion papers [LC21,CL18] can be written as

$$-\Box\Phi + s[\Phi] = \mathbf{M} \tag{105}$$

Where $s[\Phi]$ changes depending on what theory we are using. This can, in turn, be written as matrix multiplication

$$(-\Box + \mathcal{J}[\Phi])\Phi = \mathbf{M} \tag{106}$$

Using the definition of a physical law being invariant

$$F(\Phi) = g^{-1}F(g\Phi) \tag{107}$$

By inspection, we know that $g^{-1}\Box g = \Box$ for all elements in C_∞ and D_∞, next we note that in the basis where all lattice states have been rotated or reflected by some element of D_∞ the appropriate orbit Jacobian is $\mathcal{J}[g\Phi]$ with this in mind, carrying through with (107) shows that the cat map, ϕ^3, and ϕ^4 are all invariant under D_∞. Realizing that our lattice equations have inherent symmetries is extremely useful. We can utilize them to speed up calculations, and make deeper theoretical observations...as long as we understand the symmetries we are working with.

11.1. Symmetries of the square lattice

The unit cell of the integer lattice (**??**) tiles a hypercubic lattice under action of d commuting translations (**??**), called 'shifts' for infinite lattices, 'rotations' for finite periodic lattices. They form the abelian *translation group* $T = \{r_j^k \,|\, j = 1, 2, \cdots, d\,,\;\; k \in \mathbb{Z}\}$, where $r_j^0 = \mathbb{1}_j$ denotes the identity, and r_j, r_j^2, $\cdots$, r_j^k, $\cdots$, denote translations by $1, 2, \cdots, k, \cdots$ lattice sites in the jth spatiotemporal direction. For a square lattice, the translation group consists of the product of two commuting infinite cyclic groups $T = \mathrm{C}_{\infty,1} \otimes \mathrm{C}_{\infty,2}$, with

$$\mathrm{C}_{\infty,j} = \{\cdots, r_j^{-2}, r_j^{-1},\, \mathbb{1}, r_j^1, r_j^2, r_j^3, \cdots\} \tag{108}$$

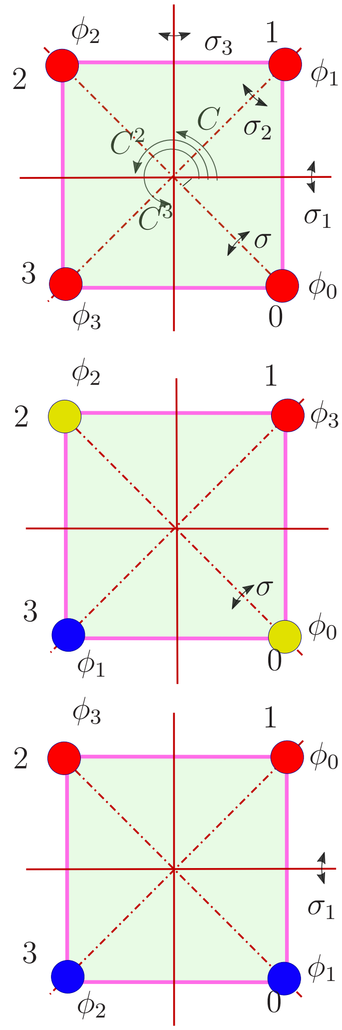

Figure 7: (Color online) Dihedral group D_4, the group of all symmetries (109) that overlie a square onto itself, consists of 3 rotations C^k that permute the sites cyclically, and 4 rotate-reflect elements σ_k that reflect the square across reflection axes, exchanging the red and the blue sites. An even reflection (long diagonal, dashed line reflection axis), here σ, leaves a pair of opposite sites fixed (marked yellow), while an odd reflection axis (short diagonal, full line), here σ_1, bisects the opposite edges, and flips all sites.

in the jth direction.

For space groups, the cosets by translation subgroup T form the *factor* (also known as *quotient*) group G/T, isomorphic to the point group g.

The Euler–Lagrange equations that define the spatiotemporal lattice field theories of section **??** are invariant under the discrete spacetime translations; the space σ_1 and time σ_3 reflections $n \to -n$, $t \to -t$; as well as under σ and σ_2 exchanges $n \longleftrightarrow t$ of space and time. They thus have the point-group symmetries of the square lattice: rotation C by $\pi/2$, reflections σ_1 across space-axis, σ_3 across time-axis, and σ_0, σ_2 across the two spacetime diagonals,

$$\mathrm{D}_4 = \{e, C, C^2, C^4, \sigma_1, \sigma_3, \sigma_0, \sigma_2\}\,, \tag{109}$$

see figure 7. In the international crystallographic notation, this square lattice space group of symmetries is referred to as *p4mm* [63].

Classifying periodic states by their factor group G/T is already not a simple undertaking in one temporal dimension (the subject of paper I), where it amounts to a purely group-theoretic reduction of the time reversal symmetry. While D_4 is the point group (109) of the unit square, each Bravais lattice (**??**) has its own factor group G/T, and -for purposes of this exposition- classifying them would lead us far from our main thrust. Here we shall construct the partition function and its reciprocal lattice representation in terms of prime periodic states, assuming only the $T = \mathrm{C}_{\infty,1} \otimes \mathrm{C}_{\infty,2}$ space and time translational invariance of system's Euler–Lagrange equations. The cost of ignoring the point-group symmetries is overcounting reflection-symmetric periodic states.

11.2. Internal symmetries

In addition to section 11.1 spacetime 'geometrical' symmetries: invariance of the shape of a periodic state under coordinate translations, rotations, and reflections, a field theory might have *internal* symmetries, groups of transformations that leave the Euler–Lagrange equations invariant, but act only on a lattice site *field*, not on site's location in the spacetime lattice.

For example, the ϕ^4 Euler–Lagrange equation (12) is invariant under the D_1 reflection $\phi_z \to -\phi_z$, and the spatiotemporal cat (10) is invariant under D_1 inversion of the field though the center of the $0 \le \phi_z < 1$ unit interval:

$$\bar{\phi}_z = 1 - \phi_z \mod 1\,, \qquad \text{for all } j \in \mathcal{L}\,, \tag{110}$$

and the corresponding inversion of lattice site symbol m_z. If $\Phi = \{\phi_z\}$ is a periodic state of the system, its inversion $\bar{\Phi} = \{\bar{\phi}_z\}$ is also a periodic state. So every periodic state of either belongs to a pair of asymmetric periodic states $\{\Phi, \bar{\Phi}\}$, or is symmetric under the inversion.

In principle, the internal symmetries should also be taken care of, but to keep the exposition simple, they are not quotiented in this paper.

11.3. What are 'periodic states'? Orbits?

For evolution-in-time, every period-n periodic point is a fixed point of the nth iterate of the 1 time-step map. In the lattice formulation, the totality of finite-period periodic states is the *set of fixed points* of all $H_{\mathbf{a}}$ and $H_{\mathbf{a},k}$ subgroups of D_∞.

Definition: Orbit *or* G-orbit *of a periodic state* Φ *is the set of all periodic states*

$$\mathcal{M}_\Phi = \{g\,\Phi \mid g \in G\} \tag{111}$$

into which Φ is mapped under the action of group G. We label the orbit $\mathcal{M}_\Phi$ by any periodic state Φ belonging to it.

Definition: Symmetry of a solution. *We shall refer to the maximal subgroup $G_\Phi \subseteq G$ of actions which permute periodic states within the orbit $\mathcal{M}_\Phi$, but leave the orbit invariant, as the* symmetry G_Φ *of the orbit $\mathcal{M}_\Phi$,*

$$G_\Phi = \{g \in G_\Phi \mid g\mathcal{M}_\Phi = \mathcal{M}_\Phi\} \,. \tag{112}$$

An orbit $\mathcal{M}_\Phi$ is G_Φ-*symmetric* (*symmetric*, *set-wise symmetric*, *self-dual*) if the action of elements of G_Φ on the set of periodic states $\mathcal{M}_\Phi$ reproduces the orbit.

Definition: Index *of orbit $\mathcal{M}_\Phi$ is given by*

$$m_\Phi = |G|/|G_\Phi| \tag{113}$$

(see Wikipedia [213] and Dummit and Foote [68]).

And now, a pleasant surprise, obvious upon an inspection of figures **??** and **??**: what happens in the primitive cell, stays in the primitive cell. Even though the lattices $\mathcal{L}$, $\mathcal{L}_\mathbf{a}$ are infinite, and their symmetries D_∞, $H_\mathbf{a}$, $H_{\mathbf{a},k}$ are *infinite* groups, the Bravais periodic states' *orbits* are *finite*, described by the finite group permutations of the infinite lattice curled up into a primitive cell periodic n-site ring.

12. Summary

How to think about matters spatiotemporal?

Acknowledgments

We are grateful to [...] . No actual cats, graduate or undergraduate were harmed during this research.

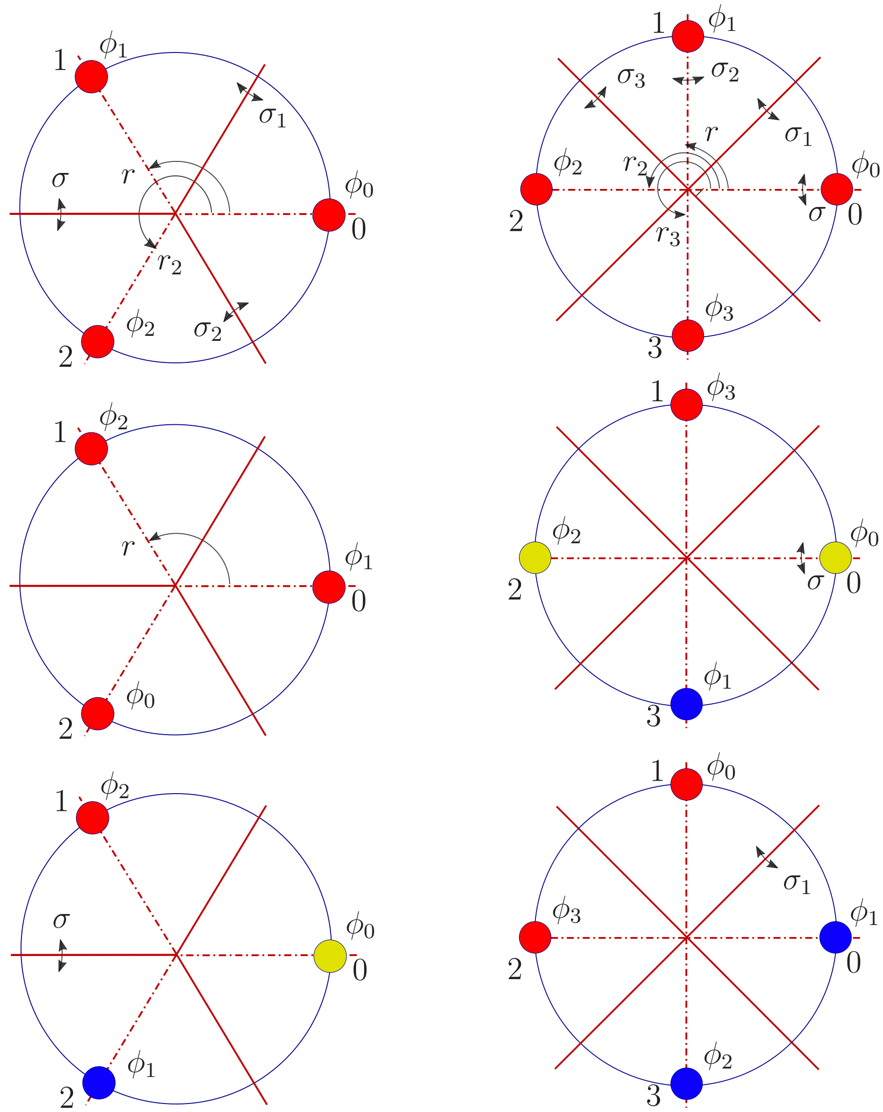

Figure 8: (Color online) Consider a period-n primitive cell tiling of a one-dimensional lattice $\mathcal{L}$. With $\mathcal{L}$ curled into a ring of n lattice sites, actions of the infinite dihedral group D_∞ reduce to translational and reflection symmetries of (D$_3$) an equilateral triangle, $n = 3$ lattice sites; (D$_4$) a square, $n = 4$ lattice sites; all group operations that overlie an n-sided regular polygon onto itself. The n translations r_j permute the sites cyclically. The n dihedral group D_n translate-reflect σ_k elements (**??**) reflect the sites across reflection axes, exchanging red and blue sites. For even n, an even reflection (dashed line reflection axis), here σ, leaves a pair of opposite sites fixed (marked yellow), while an odd reflection axis (full line), here σ_1, bisects the opposite edges, and flips all sites. For odd n, every reflection half-axis leaves a site fixed (dashed line), and bisects the opposite edge (full line). This periodic ring visualization makes it obvious that any symmetric periodic state is reflection invariant across two points on the lattice, see figure **??**.

Appendix A. Spatiotemporal Hénon

[2024-03-06 Predrag] Move to here all Hénon text previously in the Tigers' `phi3.tex`

The simplest nonlinear field theory with polynomial potential, the scalar ϕ^3 theory, turns out to be the spacetime generalization of the paradigmatic dynamicist's model of a two-dimensional nonlinear dynamical system, the quadratic Hénon map [99]

$$
\begin{aligned}
x_{t+1} &= 1 - a\,x_t^2 + b\,y_t \\
y_{t+1} &= x_t\,.
\end{aligned}
\tag{A.1}
$$

For the contraction parameter value $b = -1$ this is an area-preserving, Hamiltonian map. The Hénon map is the simplest map that captures chaos that arises from the smooth stretch & fold dynamics of nonlinear return maps of flows such as Rössler [184].

The map can be interpreted as a kicked driven anaharmonic oscillator [98], with the nonlinear, cubic Biham-Wenzel [27] lattice site potential (50)

$$
V(\phi) = \frac{1}{2}\,\mu^2\phi^2 - \frac{1}{3!}\,g\,\phi^3\,,
\tag{A.2}
$$

so we refer to this field theory as ϕ^3 theory. A parameter can be rescaled away by translations and rescalings of the field ϕ, and the Euler–Lagrange equation of the system can brought to various equivalent forms, such as the Hénon form (A.3), or the anti-integrable form (A.4),

Written as a 2nd-order inhomogeneous difference equation [67], (A.1) takes the nearest-neighbor Laplacian form, the Euler–Lagrange equation (8),

$$
-\Box\varphi_z + a\,\varphi_z^2 - 2d\,\varphi_z + 1 = 0\,.
\tag{A.3}
$$

To bring this to a form more convenient for our purposes, complete the square,

$$
-\Box\varphi_z - a\left[\left(\varphi_z + \frac{d}{a}\right)^2 - \frac{d^2+a}{a^2}\right] = 0\,,
$$

and rescale the field as $\varphi = -A\phi$,

$$
-\Box\phi_z - aA\left[\left(\phi_z + \frac{d}{aA}\right)^2 - \frac{d^2+a}{(aA)^2}\right] = 0\,.
$$

To cast this into the anti-integrable form pick a convenient set of roots, for example the symmetric pair $(1/2, -1/2)$, separated by 1. Then $(aA)^2 = 4(a + d^2)$. Calling that parameter the 'Klein-Gordon mass squared' μ^2, the Euler–Lagrange equation takes the anti-integrable form, with the potential dominating for large μ^2,

$$
-\Box\phi_z \;+\; \mu^2\,(1/4 - \phi_z^2) = 0\,.
\tag{A.4}
$$

To compare our results with the extensive, single temporal dimension, we note that the Hénon stretching parameter a in (A.3) and the Klein-Gordon mass μ^2 in (A.4) are related by

$$
\mu^2 = 2\sqrt{a+1}\,.
\tag{A.5}
$$

For a sufficiently large 'stretching parameter' a, or 'mass parameter' μ^2, the periodic states of this ϕ^3 theory are in one-to-one correspondence to the unimodal Hénon map Smale horseshoe repeller, cleanly split into the 'left', positive stretching and 'right', negative stretching lattice site field values. A plot of such horseshoe, given in, for example, ChaosBook Example 15.4, is helpfull in understanding that state space of deterministic solutions of strongly nonlinear field theories has fractal support. Devaney, Nitecki, Sterling and Meiss [59, 196, 198] have shown that the Hamiltonian Hénon map has a complete Smale horseshoe for stretching parameter a or Klein-Gordon mass μ^2 values (A.5) above

$$a > 5.699310786700\cdots\ . \tag{A.6}$$

$$\mu^2 > 5.17660536904\cdots\ . \tag{A.7}$$

In numerical [53] and analytic [72] calculations ChaosBook fixes the stretching parameter value to $a = 6$, $\mu^2 = 5.29150262213$, in order to guarantee that all 2^n periodic points $\phi = f^n(\phi)$ of the Hénon map (A.1) exist.

[2024-03-06 Predrag] Why not use $\mu^2 = 5.2$?

The symbolic dynamics is binary.

[2023-08-01 Predrag] Politi and Torcini [174] study of periodic states of spatiotemporal Hénon, a (1+1)-spacetime lattice of Hénon maps with solutions periodic both in space and time is the closest to the present investigation. They explain why the dependence of the lattice field at time ϕ_{t+1} on the two previous time steps prevents an interpretation of dynamics as the composition of a local chaotic evolution with a diffusion process. In the CML tradition, they study the weak coupling regime $\epsilon \approx 0$.

[2023-10-28 Predrag] A ϕ^3 paper for Tigers to check: Knill writes in QuantumCalculus.org: "looked at coupled standard maps which emerged when looking at extremization problems of Wilson type. The paper was called "Nonlinear dynamics from the Wilson Lagrangian". It is quite a neat variational problem to maximize the functional $\mathrm{tr}((D+im)^4)$ on some space of operators, where m is a mass parameter. This naturally leads in the simplest case to Hénon type cubic symplectic maps and in higher dimensions to coupled map lattices where one can prove the existence of bounded solutions using the anti-integrable limit of Aubry. "

References

[1] M. Akila, B. Gutkin, P. Braun, D. Waltner, and T. Guhr, "Semiclassical prediction of large spectral fluctuations in interacting kicked spin chains", Ann. Phys. **389**, 250–282 (2018).

[2] M. Akila, D. Waltner, B. Gutkin, P. Braun, and T. Guhr, "Semiclassical identification of periodic orbits in a quantum many-body system", Phys. Rev. Lett. **118**, 164101 (2017).

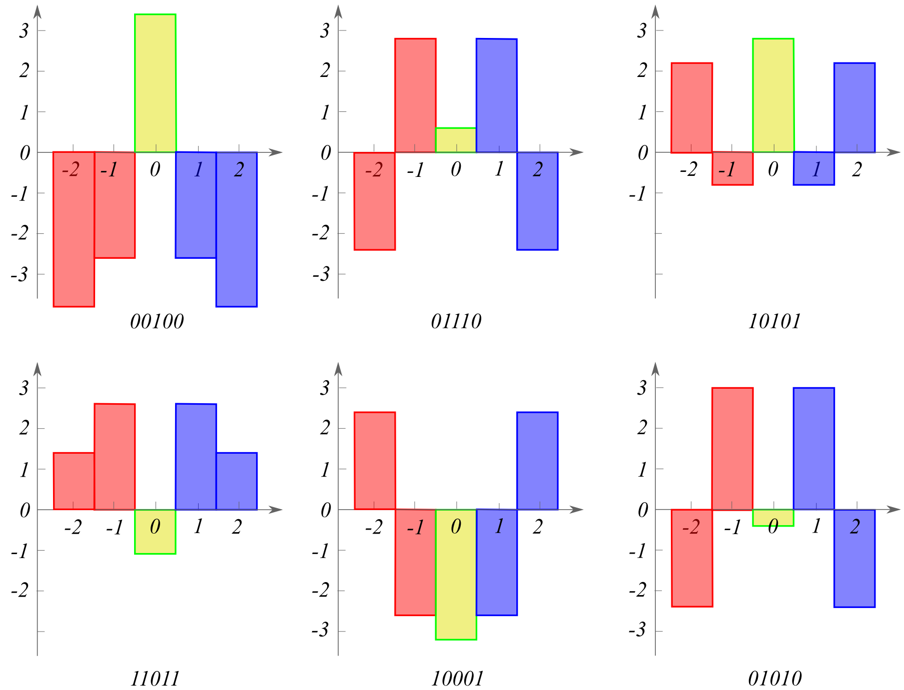

Figure A1: Temporal Hénon (**??**), $a = 6$: All period $n = 5$ prime periodic states $\overline{\phi_{-2}\phi_{-1}\boxed{\phi_0}\phi_1\phi_2}$ of table **??**. They are all reflection symmetric, with the fixed lattice field $\boxed{\phi_0}$ colored gold. The most striking feature is how far the $a = 6$ temporal Hénon is from the $0 \leftrightarrow 1$ symmetry: stretching close to $\overline{0}$ fixed point periodic state is much stronger than close to the almost marginal $\overline{1}$ fixed point periodic state. For a stretching parameter value a slight lower than the critical value $a_h = 5.69931\cdots$, the lattice sites $\boxed{\phi_0}$ for $\overline{01110}$ and $\overline{01010}$ coalesce and vanish through an inverse bifurcation. As $a \to \infty$ we expect this symmetry to be restored.

[3] M. Akila, D. Waltner, B. Gutkin, and T. Guhr, "Particle-time duality in the kicked Ising spin chain", J. Phys. A **49**, 375101 (2016).

[4] V. V. Albert, L. I. Glazman, and L. Jiang, "Topological properties of linear circuit lattices", Phys. Rev. Lett. **114**, 173902 (2015).

[5] E. Allroth, "Ground state of one-dimensional systems and fixed points of 2n-dimensional map", J. Phys. A **16**, L497 (1983).

[6] R. E. Amritkar, P. M. Gade, A. D. Gangal, and V. M. Nandkumaran, "Stability of periodic orbits of coupled-map lattices", Phys. Rev. A **44**, R3407–R3410 (1991).

[7] S. Anastassiou, A. Bountis, and A. Bäcker, "Homoclinic points of 2D and 4D maps via the parametrization method", Nonlinearity **30**, 3799–3820 (2017).

[8] W. N. Anderson and T. D. Morley, "Eigenvalues of the Laplacian of a graph", Lin. Multilin. Algebra **18**, 141–145 (1985).

[9] F. Arrigo, P. Grindrod, D. J. Higham, and V. Noferini, "On the exponential generating function for non-backtracking walks", Linear Algebra Appl. **556**, 381–399 (2018).

[10] J. H. Asad, "Differential equation approach for one- and two-dimensional lattice green's function", Mod. Phys. Lett. B **21**, 139–154 (2007).

[11] D. Atkinson and F. J. van Steenwijk, "Infinite resistive lattices", Am. J. Phys **67**, 486–492 (1999).

[12] S. Aubry, "Anti-integrability in dynamical and variational problems", Physica D **86**, 284–296 (1995).

[13] S. Aubry and G. Abramovici, "Chaotic trajectories in the standard map. The concept of anti-integrability", Physica D **43**, 199–219 (1990).

[14] M. Baake, J. Hermisson, and A. B. Pleasants, "The torus parametrization of quasiperiodic LI-classes", J. Phys. A **30**, 3029–3056 (1997).

[15] J.-C. Ban, W.-G. Hu, S.-S. Lin, and Y.-H. Lin, *Zeta Functions for Two-dimensional Shifts of Finite Type*, Vol. 221, Memoirs Amer. Math. Soc. (Amer. Math. Soc., Providence RI, 2013).

[16] R. Band, J. M. Harrison, and C. H. Joyner, "Finite pseudo orbit expansions for spectral quantities of quantum graphs", J. Phys. A **45**, 325204 (2012).

[17] A. Barvinok, *A Course in Convexity* (Amer. Math. Soc., New York, 2002).

[18] A. Barvinok, *Integer Points in Polyhedra* (European Math. Soc. Pub., Berlin, 2008).

[19] H. Bass, "The Ihara-Selberg zeta function of a tree lattice", Int. J. Math. **3**, 717–797 (1992).

[20] R. J. Baxter, "The bulk, surface and corner free energies of the square lattice Ising model", J. Phys. A **50**, 014001 (2016).

[21] M. Beck and S. Robins, *Computing the Continuous Discretely* (Springer, New York, 2007).

[22] B. Bertini, P. Kos, and T. Prosen, "Exact spectral form factor in a minimal model of many-body quantum chaos", Phys. Rev. Lett. **121**, 264101 (2018).

[23] B. Bertini, P. Kos, and T. Prosen, "Entanglement spreading in a minimal model of maximal many-body quantum chaos", Phys. Rev. X **9**, 021033 (2019).

[24] B. Bertini, P. Kos, and T. Prosen, "Exact correlation functions for dual-unitary lattice models in 1+1 dimensions", Phys. Rev. Lett. **123**, 210601 (2019).

[25] B. Bertini, P. Kos, and T. Prosen, "Operator entanglement in local quantum circuits i: Chaotic dual-unitary circuits", SciPost Physics **8**, 067 (2020).

[26] H. S. Bhat and B. Osting, "Diffraction on the two-dimensional square lattice", SIAM J. Appl. Math. **70**, 1389–1406 (2010).

[27] O. Biham and W. Wenzel, "Characterization of unstable periodic orbits in chaotic attractors and repellers", Phys. Rev. Lett. **63**, 819 (1989).

[28] P. Blanchard and D. Volchenkov, *Random Walks and Diffusions on Graphs and Databases* (Springer, Berlin, 2011).

[29] S. V. Bolotin and D. V. Treschev, "Hill's formula", Russ. Math. Surv. **65**, 191 (2010).

[30] T. Bountis and R. H. G. Helleman, "On the stability of periodic orbits of two-dimensional mappings", J. Math. Phys **22**, 1867–1877 (1981).

[31] R. Bowen, "Markov partitions for Axiom A diffeomorphisms", Amer. J. Math. **92**, 725–747 (1970).

[32] R. Bowen and O. Lanford, Zeta functions of restrictions of the shift transformation, in Global Analysis (Proc. Sympos. Pure Math., Berkeley, CA, 1968), Vol. 1, edited by S.-S. Chern and S. Smale (1970), pp. 43–50.

[33] A. Boyarsky and P. Góra, *Laws of Chaos: Invariant Measures and Dynamical Systems in One Dimension* (Birkhäuser, Boston, 1997).

[34] L. Boyle and P. J. Steinhardt, Self-similar one-dimensional quasilattices, 2016.

[35] R. B. S. Brooks, R. F. Brown, J. Pak, and D. H. Taylor, "Nielsen numbers of maps of tori", Proc. Amer. Math. Soc. **52**, 398–398 (1975).

[36] A. Brown, "Equations for periodic solutions of a logistic difference equation", J. Austral. Math. Soc. Ser. B **23**, 78–94 (1981).

[37] B. L. Buzbee, G. H. Golub, and C. W. Nielson, "On direct methods for solving Poisson's equations", SIAM J. Numer. Anal. **7**, 627–656 (1970).

[38] J. L. Cardy, "Operator content of two-dimensional conformally invariant theories", Nucl. Phys. B **270**, 186–204 (1986).

[39] M. Cencini, A. Puglisi, D. Vergni, and A. Vulpiani, *A Random Walk in Physics* (Springer, 2021).

[40] M. Chen, "On the solution of circulant linear systems", SIAM J. Numer. Anal. **24**, 668–683 (1987).

[41] G. Chinta, J. Jorgenson, and A. Karlsson, "Zeta functions, heat kernels, and spectral asymptotics on degenerating families of discrete tori", Nagoya Math. J. **198**, 121–172 (2010).

[42] G. Chinta, J. Jorgenson, and A. Karlsson, "Heat kernels on regular graphs and generalized Ihara zeta function formulas", Monatsh. Math. **178**, 171–190 (2014).

[43] S.-N. Chow, J. Mallet-Paret, and W. Shen, "Traveling waves in lattice dynamical systems", J. Diff. Equ. **149**, 248–291 (1998).

[44] S.-N. Chow, J. Mallet-Paret, and E. S. Van Vleck, "Pattern formation and spatial chaos in spatially discrete evolution equations", Random Comput. Dynam. **4**, 109–178 (1996).

[45] F. Chung and S.-T. Yau, "Discrete Green's functions", J. Combin. Theory A **91**, 19–214 (2000).

[46] D. Cimasoni, "The critical Ising model via Kac-Ward matrices", Commun. Math. Phys. **316**, 99–126 (2012).

[47] B. Clair, "The Ihara zeta function of the infinite grid", Electron. J. Combin. **21**, P2–16 (2014).

[48] B. Clair and S. Mokhtari-Sharghi, "Zeta functions of discrete groups acting on trees", J. Algebra **237**, 591–620 (2001).

[49] B. Clair and S. Mokhtari-Sharghi, "Convergence of zeta functions of graphs", Proc. Amer. Math. Soc. **130**, 1881–1887 (2002).

[50] H. Cohen, *A Course in Computational Algebraic Number Theory* (Springer, Berlin, 1993).

[51] J. Cserti, "Application of the lattice Green's function for calculating the resistance of an infinite network of resistors", Amer. J. Physics **68**, 896–906 (2000).

[52] J. Cserti, G. Széchenyi, and G. Dávid, "Uniform tiling with electrical resistors", J. Phys. A **44**, 215201 (2011).

[53] P. Cvitanović, R. Artuso, R. Mainieri, G. Tanner, and G. Vattay, *Chaos: Classical and Quantum* (Niels Bohr Inst., Copenhagen, 2023).

[54] P. Cvitanović, R. Artuso, L. Rondoni, and E. A. Spiegel, "Transporting densities", in *Chaos: Classical and Quantum*, edited by P. Cvitanović, R. Artuso, R. Mainieri, G. Tanner, and G. Vattay (Niels Bohr Inst., Copenhagen, 2023).

[55] P. Cvitanović and H. Liang, A chaotic lattice field theory in two dimensions, In preparation, 2023.

[56] F. Dannan, S. Elaydi, and P. Liu, "Periodic solutions of difference equations", J. Difference Equations and Applications **6**, 203–232 (2000).

[57] J. A. De Loera, R. Hemmecke, J. Tauzer, and R. Yoshida, "Effective lattice point counting in rational convex polytopes", J. Symbolic Comp. **38**, 1273–1302 (2004).

[58] A. Deitmar, "Ihara zeta functions of infinite weighted graphs", SIAM J. Discrete Math. **29**, 2100–2116 (2015).

[59] R. L. Devaney and Z. Nitecki, "Shift automorphisms in the Hénon mapping", Commun. Math. Phys. **67**, 137–146 (1979).

[60] A. Dienstfrey, F. Hang, and J. Huang, "Lattice sums and the two-dimensional, periodic Green's function for the Helmholtz equation", Proc. Roy. Soc. Ser A **457**, 67–85 (2001).

[61] F. W. Dorr, "The direct solution of the discrete Poisson equation on a rectangle", SIAM Rev. **12**, 248–263 (1970).

[62] P. G. Doyle and J. L. Snell, "Random walks and electric networks", in *Intelligent Systems, Control and Automation: Science and Engineering* (Springer, 2012), pp. 259–265.

[63] M. S. Dresselhaus, G. Dresselhaus, and A. Jorio, *Group Theory: Application to the Physics of Condensed Matter* (Springer, New York, 2007).

[64] D. J. Driebe, *Fully Chaotic Maps and Broken Time Symmetry* (Springer, New York, 1999).

[65] J. Dubout, Zeta functions of graphs, their symmetries and extended Catalan numbers.

[66] D. Dudgeon and R. M. Mersereau, *Multidimensional Digital Signal Processing* (Prentice-Hall, Englewood Cliffs, NJ, 1984).

[67] H. R. Dullin and J. D. Meiss, "Generalized Hénon maps: the cubic diffeomorphisms of the plane", Physica D **143**, 262–289 (2000).

[68] D. S. Dummit and R. M. Foote, *Abstract Algebra* (Wiley, 2003).

[69] E. N. Economou, *Green's Functions in Quantum Physics* (Springer, Berlin, 2006).

[70] S. Elaydi, *An Introduction to Difference Equations*, 3rd ed. (Springer, Berlin, 2005).

[71] A. Endler and J. A. C. Gallas, "Conjugacy classes and chiral doublets in the Hénon Hamiltonian repeller", Phys. Lett. A **356**, 1–7 (2006).

[72] A. Endler and J. A. C. Gallas, "Reductions and simplifications of orbital sums in a Hamiltonian repeller", Phys. Lett. A **352**, 124–128 (2006).

[73] T. Engl, J. Dujardin, A. Argüelles, P. Schlagheck, K. Richter, and J. D. Urbina, "Coherent backscattering in Fock space: A signature of quantum many-body interference in interacting bosonic systems", Phys. Rev. Lett. **112**, 140403 (2014).

[74] T. Engl, P. Plöss, J. D. Urbina, and K. Richter, "The semiclassical propagator in fermionic Fock space", Theor. Chem. Acc. **133**, 1563 (2014).

[75] T. Engl, J. D. Urbina, Q. Hummel, and K. Richter, "Complex scattering as canonical transformation: A semiclassical approach in Fock space", Ann. Phys. **527**, 737–747 (2015).

[76] T. Engl, J. D. Urbina, and K. Richter, "Periodic mean-field solutions and the spectra of discrete bosonic fields: Trace formula for Bose-Hubbard models", Phys. Rev. E **92**, 062907 (2015).

[77] T. Engl, J. D. Urbina, and K. Richter, "The semiclassical propagator in Fock space: dynamical echo and many-body interference", Philos. Trans. Royal Soc. A **374**, 20150159 (2016).

[78] A. L. Fetter and J. D. Walecka, *Theoretical Mechanics of Particles and Continua* (Dover, New York, 2003).

[79] M. Fiedler, "Algebraic connectivity of graphs", Czech. Math. J **23**, 298–305 (1973).

[80] D. Fischer, G. Golub, O. Hald, C. Leiva, and O. Widlund, "On Fourier-Toeplitz methods for separable elliptic problems", Math. Comput. **28**, 349–349 (1974).

[81] L. Flatto, J. C. Lagarias, and B. Poonen, "The zeta function of the beta transformation", Ergodic Theory Dynam. Systems **14**, 237–266 (1994).

[82] F. Flicker, "Time quasilattices in dissipative dynamical systems", SciPost Phys. **5**, 001 (2018).

[83] E. Fradkin, *Field Theories of Condensed Matter Physics* (Cambridge Univ. Press, Cambridge UK, 2013).

[84] S. Friedland and J. Milnor, "Dynamical properties of plane polynomial automorphisms", Ergodic Theory Dynam. Systems **9**, 67–99 (1989).

[85] P. M. Gade and R. E. Amritkar, "Spatially periodic orbits in coupled-map lattices", Phys. Rev. E **47**, 143–154 (1993).

[86] R. Giles and C. B. Thorn, "Lattice approach to string theory", Phys. Rev. D **16**, 366–386 (1977).

[87] J. I. Glaser, "Numerical solution of waveguide scattering problems by finite-difference Green's functions", IEEE Trans. Microwave Theory Tech. **18**, 436–443 (1970).

[88] C. Godsil and G. F. Royle, *Algebraic Graph Theory* (Springer, New York, 2013).

[89] G. H. Golub and C. F. Van Loan, *Matrix Computations*, 4th ed. (J. Hopkins Univ. Press, Baltimore, MD, 2013).

[90] G. Grimmett, *Probability on Graphs: : Random Processes on Graphs and Lattices* (Cambridge Univ. Press, 2009).

[91] D. Guido, T. Isola, and M. L. Lapidus, "A trace on fractal graphs and the Ihara zeta function", Trans. Amer. Math. Soc. **361**, 3041–3041 (2009).

[92] B. Gutkin, L. Han, R. Jafari, A. K. Saremi, and P. Cvitanović, "Linear encoding of the spatiotemporal cat map", Nonlinearity **34**, 2800–2836 (2021).

[93] B. Gutkin and V. Osipov, "Classical foundations of many-particle quantum chaos", Nonlinearity **29**, 325–356 (2016).

[94] A. J. Guttmann, "Lattice Green's functions in all dimensions", J. Phys. A **43**, 305205 (2010).

[95] K. T. Hansen, "Alternative method to find orbits in chaotic systems", Phys. Rev. E **52**, 2388–2391 (1995).

[96] P. G. Harper, "Single band motion of conduction electrons in a uniform magnetic field", Proc. Phys. Soc. London, Sect. A **68**, 874–878 (1955).

[97] K. Hashimoto, "Zeta functions of finite graphs and representations of p-adic groups", Adv. Stud. Pure Math. **15**, 211–280 (1989).

[98] J. F. Heagy, "A physical interpretation of the Hénon map", Physica D **57**, 436–446 (1992).

[99] M. Hénon, "A two-dimensional mapping with a strange attractor", Commun. Math. Phys. **50**, 94–102 (1976).

[100] D. L. Hitzl and F. Zele, "An exploration of the Hénon quadratic map", Physica D **14**, 305–326 (1985).

[101] H. Hobrecht and F. Hucht, "Anisotropic scaling of the two-dimensional Ising model I: the torus", SciPost Phys. **7**, 026 (2019).

[102] H. Hobrecht and F. Hucht, "Anisotropic scaling of the two-dimensional Ising model II: surfaces and boundary fields", SciPost Phys. **8**, 032 (2020).

[103] F. Hofbauer and G. Keller, "Zeta-functions and transfer-operators for piecewise linear transformations", J. Reine Angew. Math. (Crelle) **1984**, 100–113 (1984).

[104] D. R. Hofstadter, "Energy levels and wave functions of Bloch electrons in rational and irrational magnetic fields", Phys. Rev. B **14**, 2239–2249 (1976).

[105] T. Horiguchi, "Lattice Green's function for the simple cubic lattice", J. Phys. Soc. Jpn. **30**, 1261–1272 (1971).

[106] T. Horiguchi and T. Morita, "Note on the lattice Green's function for the simple cubic lattice", J. Phys. C **8**, L232 (1975).

[107] M. D. Horton, "Ihara zeta functions of digraphs", Linear Algebra Appl. **425**, 130–142 (2007).

[108] G. Y. Hu and R. F. O'Connell, "Analytical inversion of symmetric tridiagonal matrices", J. Phys. A **29**, 1511 (1996).

[109] G. Y. Hu, J. Y. Ryu, and R. F. O'Connell, "Analytical solution of the generalized discrete Poisson equation", J. Phys. A **31**, 9279 (1998).

[110] A. Hucht, "The square lattice Ising model on the rectangle I: finite systems", J. Phys. A **50**, 065201 (2017).

[111] B. D. Hughes, *Random Walks and Random Environments: Vol. I, Random Walks* (Clarendon Press, Oxford, 1995).

[112] C. A. Hurst and H. S. Green, "New solution of the Ising problem for a rectangular lattice", J. Chem. Phys. **33**, 1059–1062 (1960).

[113] Y. Ihara, "On discrete subgroups of the two by two projective linear group over p-adic fields", J. Math. Soc. Japan **18**, 219–235 (1966).

[114] E. V. Ivashkevich, N. S. Izmailian, and C.-K. Hu, "Kronecker's double series and exact asymptotic expansions for free models of statistical mechanics on torus", J. Phys. A **35**, 5543–5561 (2002).

[115] N. S. Izmailian, "Finite-size effects for anisotropic 2D Ising model with various boundary conditions", J. Phys. A **45**, 494009 (2012).

[116] N. S. Izmailian and C.-K. Hu, "Finite-size effects for the Ising model on helical tori", Phys. Rev. E **76**, 041118 (2007).

[117] N. S. Izmailian, K. B. Oganesyan, and C.-K. Hu, "Exact finite-size corrections for the square-lattice Ising model with Brascamp-Kunz boundary conditions", Phys. Rev. E **65**, 056132 (2002).

[118] K. Jansen, "Lattice field theory", Int. J. Mod. Phys. E **16**, 2638–2679 (2007).

[119] J. Jorgenson and S. Lang, "The ubiquitous heat kernel", in *Mathematics Unlimited - 2001 and Beyond* (Springer, Berlin, 2001), pp. 655–683.

[120] L. P. Kadanoff, *Statistical Physics: Statics, Dynamics and Renormalization* (World Scientific, Singapore, 2000).

[121] G. Kane, *Modern Elementary Particle Physics* (Addison-Wesley, Redwood City, 1987).

[122] A. Karlsson and M. Neuhauser, "Heat kernels, theta identities, and zeta functions on cyclic groups", Contemp. Math. **394**, 177–190 (2006).

[123] S. Katsura and S. Inawashiro, "Lattice Green's functions for the rectangular and the square lattices at arbitrary points", J. Math. Phys. **12**, 1622–1630 (1971).

[124] S. Katsura, S. Inawashiro, and Y. Abe, "Lattice Green's function for the simple cubic lattice in terms of a Mellin-Barnes type integral", J. Math. Phys. **12**, 895–899 (1971).

[125] S. Katsura, T. Morita, S. Inawashiro, T. Horiguchi, and Y. Abe, "Lattice Green's function. Introduction", J. Math. Phys. **12**, 892–895 (1971).

[126] B. Kaufman, "Crystal statistics. II. Partition function evaluated by spinor analysis", Phys. Rev. **76**, 1232–1243 (1949).

[127] V. Khoromskaia and B. N. Khoromskij, "Block circulant and Toeplitz structures in the linearized Hartree-Fock equation on finite lattices: Tensor approach", Comput. Methods Appl. Math. **17**, 43–455 (2017).

[128] Y.-O. Kim, J. Lee, and K. K. Park, "A zeta function for flip systems", Pacific J. Math. **209**, 289–301 (2003).

[129] G. Kirchhoff, "Üeber die Auflösung der Gleichungen, auf welche man bei der Untersuchung der linearen Vertheilung galvanischer Ströme geführt wird", Ann. Phys. Chem. **148**, 497–508 (1847).

[130] O. Knill and F. Tangerman, "Self-similarity and growth in Birkhoff sums for the golden rotation", Nonlinearity **24**, 3115–3127 (2011).

[131] M. Kotani and T. Sunada, "Zeta functions of finite graphs", J. Math. Sci. Univ. Tokyo **7**, 7–25 (2000).

[132] S. Lang, *Linear Algebra* (Addison-Wesley, Reading, MA, 1987).

[133] C. H. Lee, S. Imhof, C. Berger, F. Bayer, J. Brehm, L. W. Molenkamp, T. Kiessling, and R. Thomale, "Topolectrical circuits", Commun. Phys. **1**, 39 (2018).

[134] D. Lenz, F. Pogorzelski, and M. Schmidt, "The Ihara zeta function for infinite graphs", Trans. Amer. Math. Soc. **371**, 5687–5729 (2018).

[135] S. Levit and U. Smilansky, "A new approach to Gaussian path integrals and the evaluation of the semiclassical propagator", Ann. Phys. **103**, 198–207 (1977).

[136] S. Levit and U. Smilansky, "A theorem on infinite products of eigenvalues of Sturm-Liouville type operators", Proc. Amer. Math. Soc. **65**, 299–299 (1977).

[137] H. Liang and P. Cvitanović, "A chaotic lattice field theory in one dimension", J. Phys. A **55**, 304002 (2022).

[138] T. M. Liaw, M. C. Huang, Y. L. Chou, S. C. Lin, and F. Y. Li, "Partition functions and finite-size scalings of Ising model on helical tori", Phys. Rev. E **73**, 041118 (2006).

[139] W. J. Lick, *Difference Equations from Differential Equations* (Springer, Berlin, 1989).

[140] J. S. Lim, *Two-dimensional Signal and Image Processing* (Prentice Hall, Englewood Cliffs, N.J, 1990).

[141] D. Lind and K. Schmidt, "Symbolic and algebraic dynamical systems", in *Handbook of Dynamical Systems*, Vol. 1, edited by B. Hasselblatt and A. Katok (Elsevier, New York, 2002), pp. 765–812.

[142] D. A. Lind, "A zeta function for Z^d-actions", in *Ergodic Theory of Z^d Actions*, edited by M. Pollicott and K. Schmidt (Cambridge Univ. Press, 1996), pp. 433–450.

[143] D. A. Lind and B. Marcus, *An Introduction to Symbolic Dynamics and Coding* (Cambridge Univ. Press, Cambridge, 1995).

[144] R. de la Llave, Variational methods for quasiperiodic solutions of partial differential equations, in Hamiltonian Systems and Celestial Mechanics (HAMSYS–98), edited by J. Delgado, E. A. Lacomba, E. Pérez-Chavela, and J. Llibre (2000).

[145] M. Lüscher and P. Weisz, "Scaling laws and triviality bounds in the lattice ϕ^4 theory (I). One-component model in the symmetric phase", Nucl. Phys. B **290**, 25–60 (1987).

[146] I. Lyberg, "Free energy of the anisotropic Ising lattice with Brascamp-Kunz boundary conditions", Phys. Rev. E **87**, 062141 (2013).

[147] R. S. MacKay, *Renormalisation in Area-preserving Maps* (World Scientific, Singapore, 1993).

[148] R. S. MacKay and J. D. Meiss, "Linear stability of periodic orbits in Lagrangian systems", Phys. Lett. A **98**, 92–94 (1983).

[149] J. Mallet-Paret and S.-N. Chow, "Pattern formation and spatial chaos in lattice dynamical systems. I", IEEE Trans. Circuits Systems I Fund. Theory Appl. **42**, 746–751 (1995).

[150] J. Mallet-Paret and S.-N. Chow, "Pattern formation and spatial chaos in lattice dynamical systems. II", IEEE Trans. Circuits Systems I Fund. Theory Appl. **42**, 752–756 (1995).

[151] E. C. Marino, *Quantum Field Theory Approach to Condensed Matter Physics* (Cambridge Univ. Press, Cambridge UK, 2017).

[152] P. A. Martin, "Discrete scattering theory: Green's function for a square lattice", Wave Motion **43**, 619–629 (2006).

[153] B. M. McCoy and T. T. Wu, *The Two-Dimensional Ising Model*, 2nd ed. (Dover, 1973).

[154] B. D. Mestel and I. Percival, "Newton method for highly unstable orbits", Physica D **24**, 172 (1987).

[155] H. B. Meyer, "Lattice QCD: A brief introduction", in *Lattice QCD for Nuclear Physics*, edited by H.-W. Lin and H. B. Meyer (Springer, York New, 2015), pp. 1–34.

[156] D. Micciancio and S. Goldwasser, *Complexity of Lattice Problems - A Cryptographic Perspective* (Springer, New York, 2002).

[157] M. Michałek and B. Sturmfels, *Invitation to Nonlinear Algebra* (MPI Leipzig, 2020).

[158] N. Miguel, C. Simó, and A. Vieiro, "From the Hénon conservative map to the Chirikov standard map for large parameter values", Regul. Chaotic Dyn. **18**, 469–489 (2013).

[159] R. Miles, "A dynamical zeta function for group actions", Monatsh. Math. **182**, 683–708 (2016).

[160] I. Montvay and G. Münster, *Quantum Fields on a Lattice* (Cambridge Univ. Press, Cambridge, 1994).

[161] T. Morita, "Useful procedure for computing the lattice Green's function - square, tetragonal, and bcc lattices", J. Math. Phys. **12**, 1744–1747 (1971).

[162] T. Morita and T. Horiguchi, "Calculation of the lattice Green's function for the bcc, fcc, and rectangular lattices", J. Math. Phys. **12**, 986–992 (1971).

[163] G. Münster, "Lattice quantum field theory", Scholarpedia **5**, 8613 (2010).

[164] G. Münster and M. Walzl, Lattice gauge theory - A short primer, 2000.

[165] J. Nielsen, "Über die Minimalzahl der Fixpunkte bei den Abbildungstypen der Ringflächen", Math. Ann. **82**, 83–93 (1920).

[166] J. Ningyuan, C. Owens, A. Sommer, D. Schuster, and J. Simon, "Time- and site-resolved dynamics in a topological circuit", Phys. Rev. X **5**, 021031 (2015).

[167] Y. Okabe, K. Kaneda, M. Kikuchi, and C.-K. Hu, "Universal finite-size scaling functions for critical systems with tilted boundary conditions", Phys. Rev. E **59**, 1585–1588 (1999).

[168] L. Onsager, "Crystal statistics. I. A Two-dimensional model with an order-disorder transition", Phys. Rev. **65**, 117–149 (1944).

[169] G. Papathanasiou and C. B. Thorn, "Worldsheet propagator on the lightcone worldsheet lattice", Phys. Rev. D **87**, 066005 (2013).

[170] W. Parry, "On the β-expansions of real numbers", Acta Math. Acad. Sci. Hung. **11**, 401–416 (1960).

[171] R. Peierls, "Zur Theorie des Diamagnetismus von Leitungselektronen", Z. Phys. **80**, 763–791 (1933).

[172] I. Percival and F. Vivaldi, "A linear code for the sawtooth and cat maps", Physica D **27**, 373–386 (1987).

[173] A. Poghosyan, N. Izmailian, and R. Kenna, "Exact solution of the critical Ising model with special toroidal boundary conditions", Phys. Rev. E **96**, 062127 (2017).

[174] A. Politi and A. Torcini, "Periodic orbits in coupled Hénon maps: Lyapunov and multifractal analysis", Chaos **2**, 293–300 (1992).

[175] A. Politi, A. Torcini, and S. Lepri, "Lyapunov exponents from node-counting arguments", J. Phys. IV **8**, 263 (1998).

[176] M. Pollicott, Dynamical zeta functions, in Smooth Ergodic Theory and Its Applications, Vol. 69, edited by A. Katok, R. de la Llave, Y. Pesin, and H. Weiss (2001), pp. 409–428.

[177] C. Pozrikidis, *An Introduction to Grids, Graphs, and Networks* (Oxford Univ. Press, Oxford , UK, 2014).

[178] L. Qi, H. Chen, and Y. Chen, *Tensor Eigenvalues and Their Applications* (Springer, Singapore, 2018).

[179] P. Ramond, *Field Theory* (Routledge, 1981).

[180] P. Ren, T. Aleksić, D. Emms, R. C. Wilson, and E. R. Hancock, "Quantum walks, Ihara zeta functions and cospectrality in regular graphs", Quantum Inf. Process. **10**, 405–417 (2010).

[181] A. Rényi, "Representations for real numbers and their ergodic properties", Acta Math. Acad. Sci. Hung. **8**, 477–493 (1957).

[182] M. Rezghi and L. Eldén, "Diagonalization of tensors with circulant structure", Linear Algebra Appl. **435**, 422–447 (2011).

[183] K. Richter, J. D. Urbina, and S. Tomsovic, "Semiclassical roots of universality in many-body quantum chaos", J. Phys. A **55**, 453001 (2022).

[184] O. E. Rössler, "An equation for continuous chaos", Phys. Lett. A **57**, 397–398 (1976).

[185] H. J. Rothe, *Lattice Gauge Theories - An Introduction* (World Scientific, Singapore, 2005).

[186] I. Sato, "Bartholdi zeta functions of group coverings of digraphs", Far East J. Math. Sci. **18**, 321–339 (2005).

[187] J.-P. Serre, *Trees* (Springer, Berlin, 1980).

[188] R. Shankar, *Quantum Field Theory and Condensed Matter* (Cambridge Univ. Press, Cambridge UK, 2017).

[189] C. L. Siegel and K. Chandrasekharan, *Lectures on the Geometry of Numbers* (Springer Berlin Heidelberg, Berlin, Heidelberg, 1989).

[190] C. Simó, "On the Hénon-Pomeau attractor", J. Stat. Phys. **21**, 465–494 (1979).

[191] B. Simon, "Almost periodic Schrödinger operators: A review", Adv. Appl. Math. **3**, 463–490 (1982).

[192] J. Smit, *Introduction to Quantum Fields on a Lattice* (Cambridge Univ. Press, Cambridge, 2002).

[193] R. Sommer, Introduction to Lattice Gauge Theories, tech. rep. (Humboldt Univ., 2015).

[194] H. M. Stark and A. A. Terras, "Zeta functions of finite graphs and coverings", Adv. Math. **121**, 124–165 (1996).

[195] J. Stephenson and D. T. Ridgway, "Formulae for cycles in the Mandelbrot set II", Physica A **190**, 104–116 (1992).

[196] D. Sterling and J. D. Meiss, "Computing periodic orbits using the anti-integrable limit", Phys. Lett. A **241**, 46–52 (1998).

[197] D. G. Sterling, Anti-integrable Continuation and the Destruction of Chaos, PhD thesis (Univ. Colorado, Boulder, CO, 1999).

[198] D. G. Sterling, H. R. Dullin, and J. D. Meiss, "Homoclinic bifurcations for the Hénon map", Physica D **134**, 153–184 (1999).

[199] I. Stewart and D. Gökaydin, "Symmetries of quotient networks for doubly periodic patterns on the square lattice", Int. J. Bifur. Chaos **29**, 1930026 (2019).

[200] R. Suarez, "Difference equations and a principle of double induction", Math. Mag. **62**, 334–339 (1989).

[201] T. Sunada, *Topological Crystallography* (Springer, Tokyo, 2013).

[202] A. Tarfulea and R. Perlis, "An Ihara formula for partially directed graphs", Linear Algebra Appl. **431**, 73–85 (2009).

[203] A. Terras, *Zeta Functions of Graphs: A Stroll through the Garden* (Cambridge Univ. Press, 2010).

[204] M. Toda, *Theory of Nonlinear Lattices* (Springer, Berlin, 1989).

[205] J. H. Van Vleck, "The correspondence principle in the statistical interpretation of quantum mechanics", Proc. Natl. Acad. Sci. **14**, 178–188 (1928).

[206] G. Venezian, "On the resistance between two points on a grid", Am. J. Phys **62**, 1000–1004 (1994).

[207] Y. Colin de Verdière, "Spectrum of the Laplace operator and periodic geodesics: thirty years after", Ann. Inst. Fourier **57**, 2429–2463 (2007).

[208] D. Viswanath, "The Lindstedt-Poincaré technique as an algorithm for finding periodic orbits", SIAM Rev. **43**, 478–496 (2001).

[209] D. Viswanath, "Symbolic dynamics and periodic orbits of the Lorenz attractor", Nonlinearity **16**, 1035–1056 (2003).

[210] D. Viswanath, "The fractal property of the Lorenz attractor", Physica D **190**, 115–128 (2004).

[211] U.-J. Wiese, An Introduction to Lattice Field Theory, tech. rep. (Univ. Bern, 2009).

[212] I. Wigman, "Counting singular matrices with primitive row vectors", Monatsh. Math. **144**, 71–84 (2005).

[213] Wikipedia contributors, Index of a subgroup — Wikipedia, The Free Encyclopedia, 2022.

[214] H. S. Wilf, *Generatingfunctionology* (Academic Press, New York, 1994).

[215] S. V. Williams, X. Wang, H. Liang, and P. Cvitanović, Nonlinear chaotic lattice field theory, In preparation, 2023.

[216] U. Wolff, "Triviality of four dimensional ϕ^4 theory on the lattice", Scholarpedia **9**, 7367 (2014).

[217] W. L. Wood, "Periodicity effects on the iterative solution of elliptic difference equations", SIAM J. Numer. Anal. **8**, 439–464 (1971).

[218] J. Woods, *Multidimensional Signal, Image, and Video Processing and Coding* (Academic Press, Amsterdam, 2012).

[219] F. Y. Wu, "Theory of resistor networks: the two-point resistance", J. Phys. A **37**, 6653–6673 (2004).

[220] M.-C. Wu and C.-K. Hu, "Exact partition functions of the Ising model on M x N planar lattices with periodic-aperiodic boundary conditions", J. Phys. A **35**, 5189–5206 (2002).

[221] Z.-J. Xie, X.-Q. Jin, and Y.-M. Wei, "A fast algorithm for solving circulant tensor systems", Lin. Multilin. Algebra **65**, 1894–1904 (2016).

[222] Y. Yamasaki, "An explicit prime geodesic theorem for discrete tori and the hypergeometric functions", Math. Z. **289**, 361–376 (2017).

[223] Q. Zhilin, A. Gangal, M. Benkun, and T. Gang, "Spatiotemporally periodic patterns in symmetrically coupled map lattices", Phys. Rev. E **50**, 163–170 (1994).

[224] D. Zhou, Y. Xiao, and Y.-H. He, "Seiberg duality, quiver gauge theories, and Ihara's zeta function", Int. J. Mod. Phys. A **30**, 1550118 (2015).

[225] R. M. Ziff, C. D. Lorenz, and P. Kleban, "Shape-dependent universality in percolation", Physica A **266**, 17–26 (1999).